Advances in many-body theory and applications to heavy-ion collisions

Dean Lee
Facility for Rare Isotope Beams
Michigan State University
Nuclear Lattice EFT Collaboration

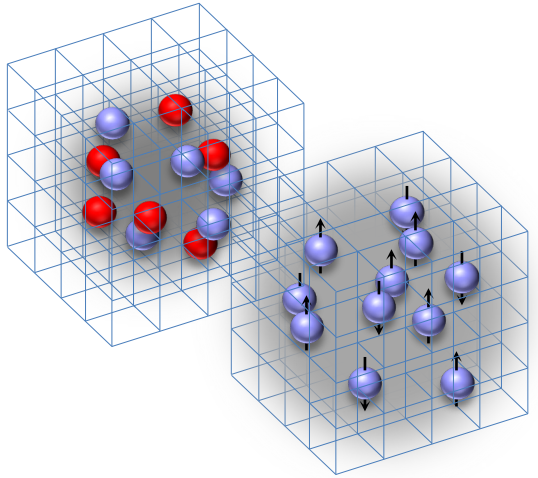

CERN Theory Colloquium
Light Ion Collisions at the LHC Workshop
November 13, 2024

FRIB
MICHIGAN STATE UNIVERSITY
NUCLEI
Nuclear Computational Low-Energy Initiative
A SciDAC-4 Project
JÜLICH FORSCHUNGSZENTRUM
OAK RIDGE National Laboratory | LEADERSHIP COMPUTING FACILITY

Outline

Light ion collisions at the LHC

Ab initio methods

Nuclear lattice effective field theory (NLEFT)

Essential elements for nuclear binding

Pinhole algorithm

Emergent geometry and duality of ^{12}C

Recent advances using NLEFT

^{16}O^{16}O collisions

^{16}O^{16}O versus ^{20}Ne^{20}Ne collisions

^{208}Pb^{16}O versus ^{208}Pb^{20}Ne collisions

Summary and outlook


Light ion collisions at the LHC
Location: 4/3-006, CERN
Website: cern.ch/lightions
Date: Nov. 11-15, 2024
Topics covered in relation to small systems:
Experimental highlights and projections
Heavy flavour
Hydrodynamics
Initial conditions
Jets
Ultraperipheral collisions
Nuclear parton distribution functions
Nuclear structure
LHC accelerator opportunities
Organisers:
Reyes Alemany Fernandez
Giuliano Giacalone
Qipeng Hu
Govert Hugo Nijs
Saverio Mariani
Wilke van der Schee
Huichao Song
Jing Wang
Urs Wiedemann
You Zhou

Heavy-Ion Collisions

Dynamical description of Heavy-Ion collisions from underlying theory of QCD remains an outstanding challenge

Standard model of nucleus-nucleus (A+A) collisions based on effective macroscopic descriptions of QCD

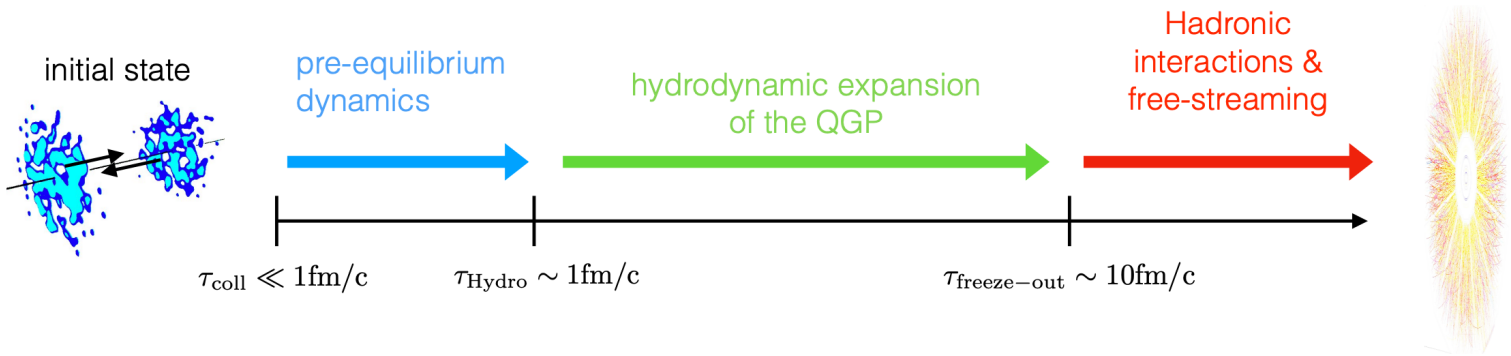

Quantitatively accurate description of soft physics observables in HICs

Significant theoretical progress in dynamical description of early stages

Schlichting, Wednesday, November 13

Flow harmonics in heavy-ion collisions

$$v_n = \langle \cos[n(\phi - \psi_n)] \rangle$$

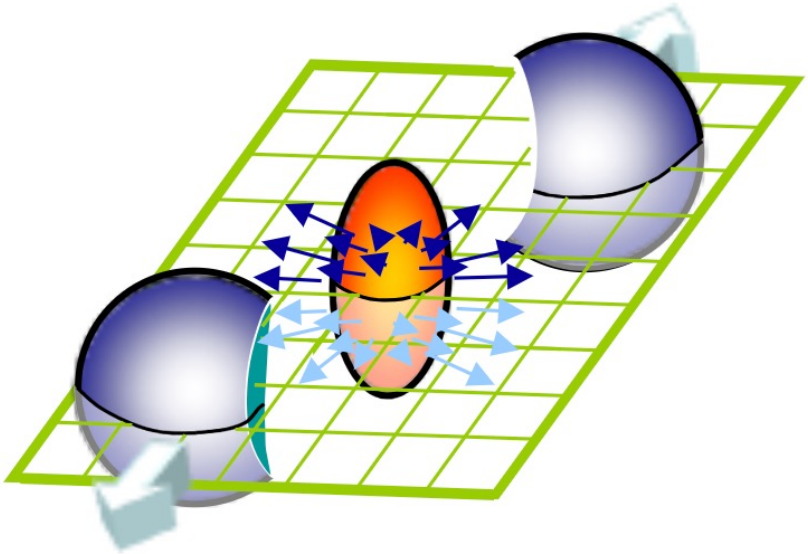

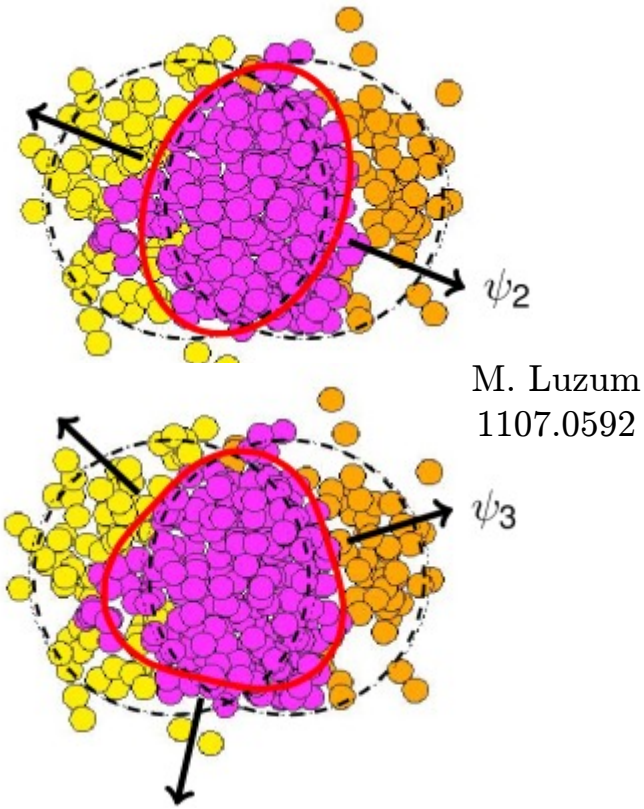

M. Luzum
1107.0592

Pressure gradients

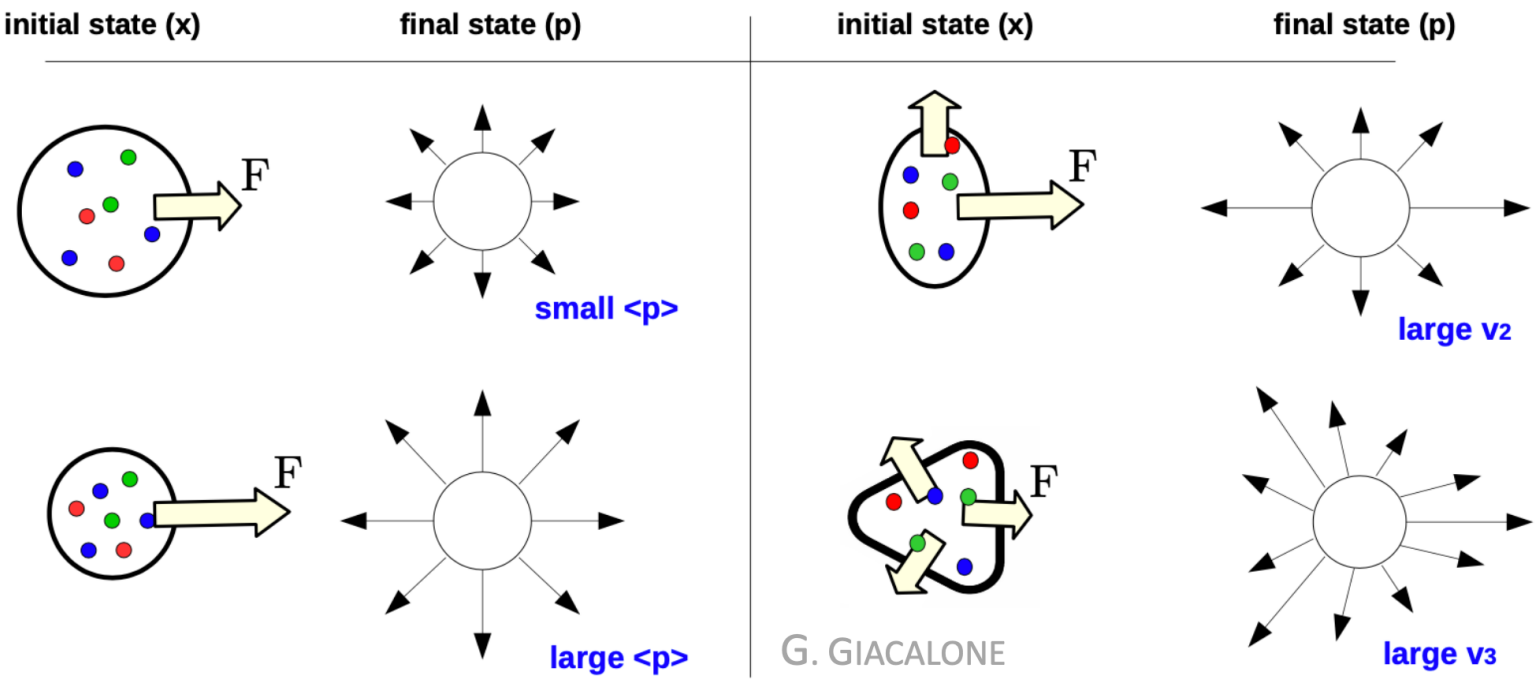

Nuclear structure

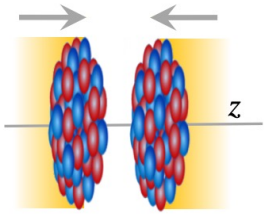

Initial condition

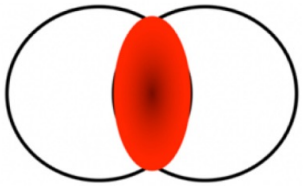

Final state

hydrodynamics

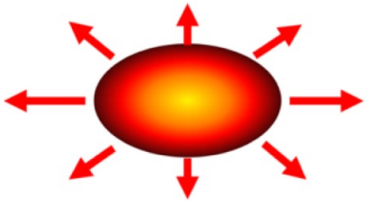

Shape and radial dis.

$\beta_2 \rightarrow$ Quadrupole deformation
$\beta_3 \rightarrow$ Octupole deformation
$a_0 \rightarrow$ Surface diffuseness
$R_0 \rightarrow$ Nuclear size

Volume, size and shape

$$N_{\rm part}$$
$$R_\perp^2 \propto \langle r_\perp^2 \rangle$$
$$\mathcal{E}_n \propto \langle r_\perp^n e^{in\phi} \rangle$$

Observables

$$\frac{d^2N}{d\phi dp_T} = N(p_T)\left(\sum_n V_{\rm n}\, e^{-in\phi}\right)$$

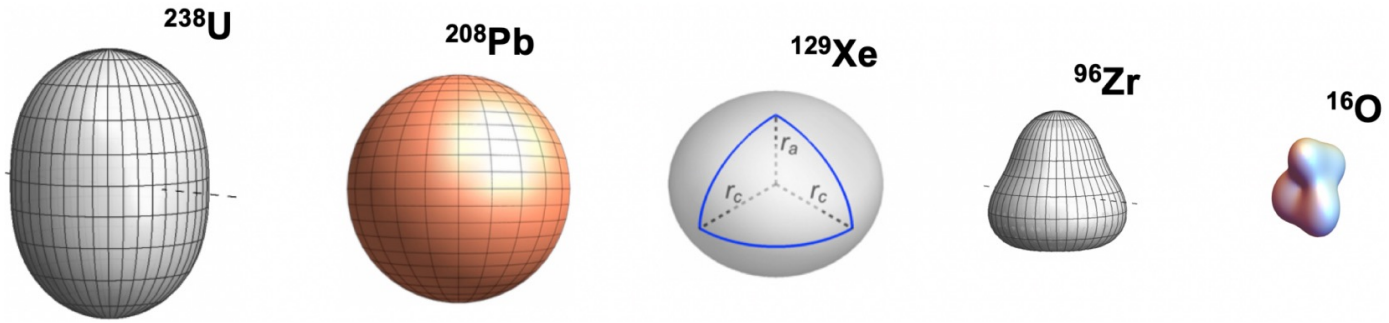

Jia and Giacalone, QM 2023

Multi-faceted interest in light ions

So far, strong qualitative indication of "hydrodynamic behavior"

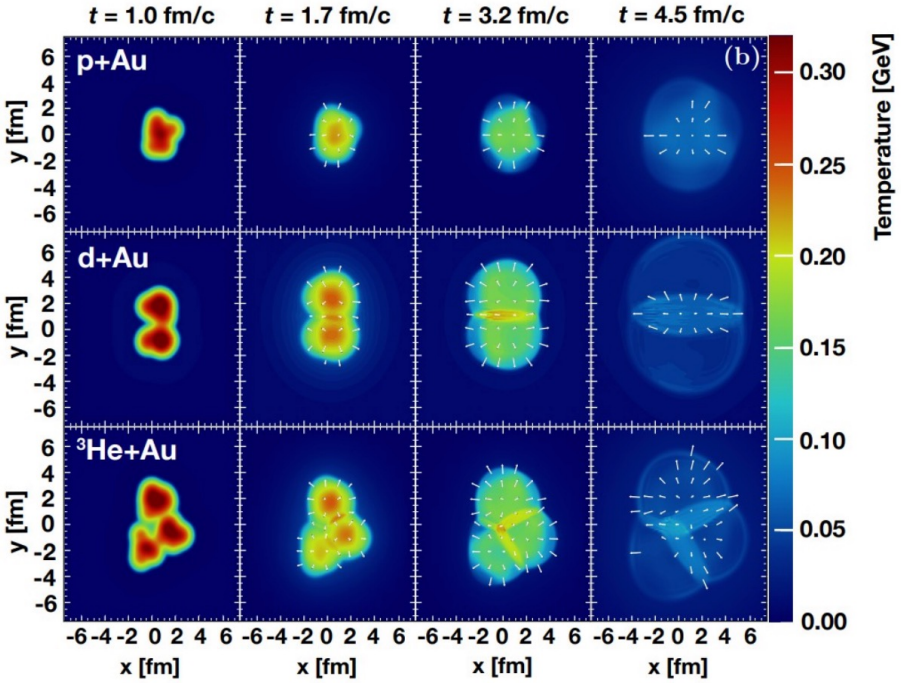

$$v_2\{2\}_{d^{197}\mathrm{Au}} > v_2\{2\}_{p^{197}\mathrm{Au}}$$

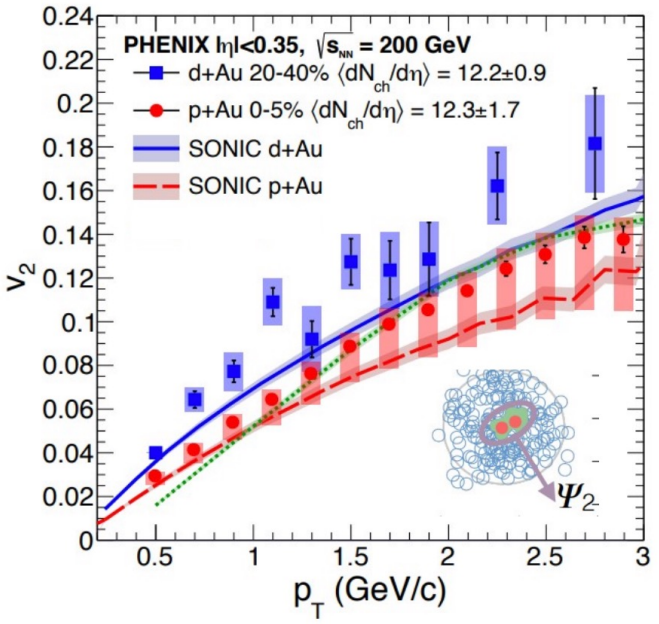

[PHENIX Collaboration, Nature Phys. **15** (2019) 3, 214-220]
[STAR collaboration, PRL **130** (2023) 242301]

Giacalone, Monday, Nov. 11

A-dependence of nuclear modifications

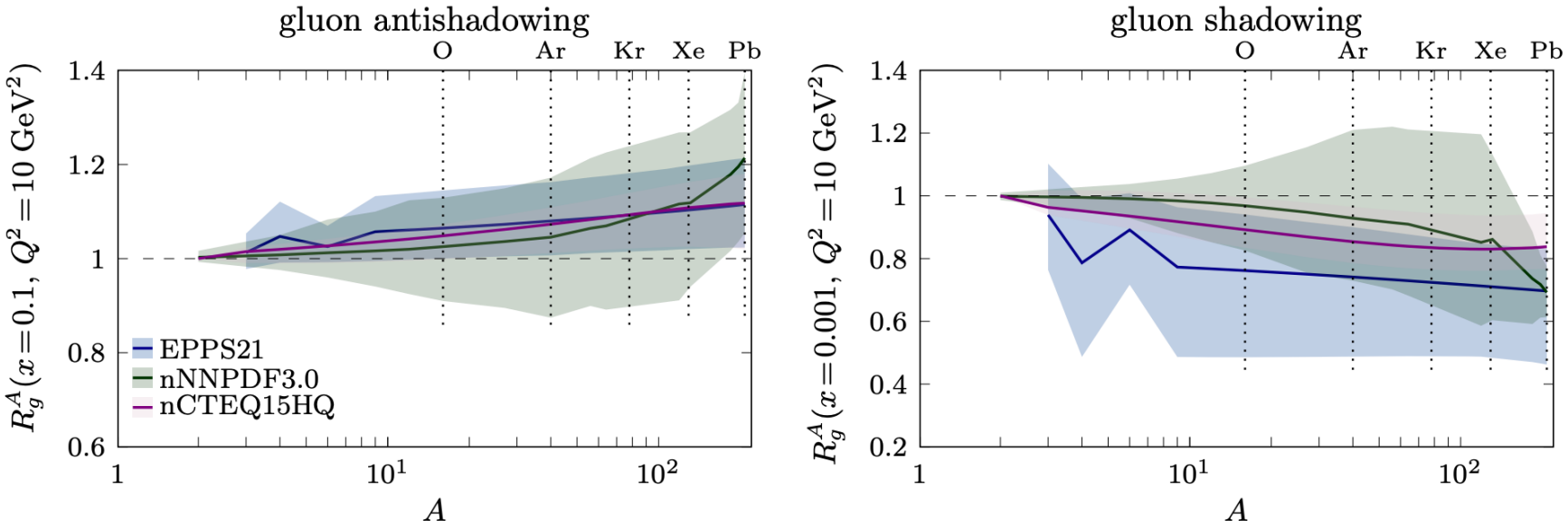

A-dependence of gluon PDFs not well constrained by data!

- Having data for even one additional nucleus would help interpolating the effect for others (but note that A-dependence is not necessarily smooth or even monotonous)
- Nuclear PDFs a major source of uncertainty for testing existence of QGP in small systems

Huss et al., PRL 126 (2021) 192301
Brewer, Huss, Mazeliauskas, van der Schee, PRD 105 (2022) 074040
Gebhard, Mazeliauskas, Takacs, arXiv:2410.22405 [hep-ph]

Paakkinen, Tuesday, Nov. 12

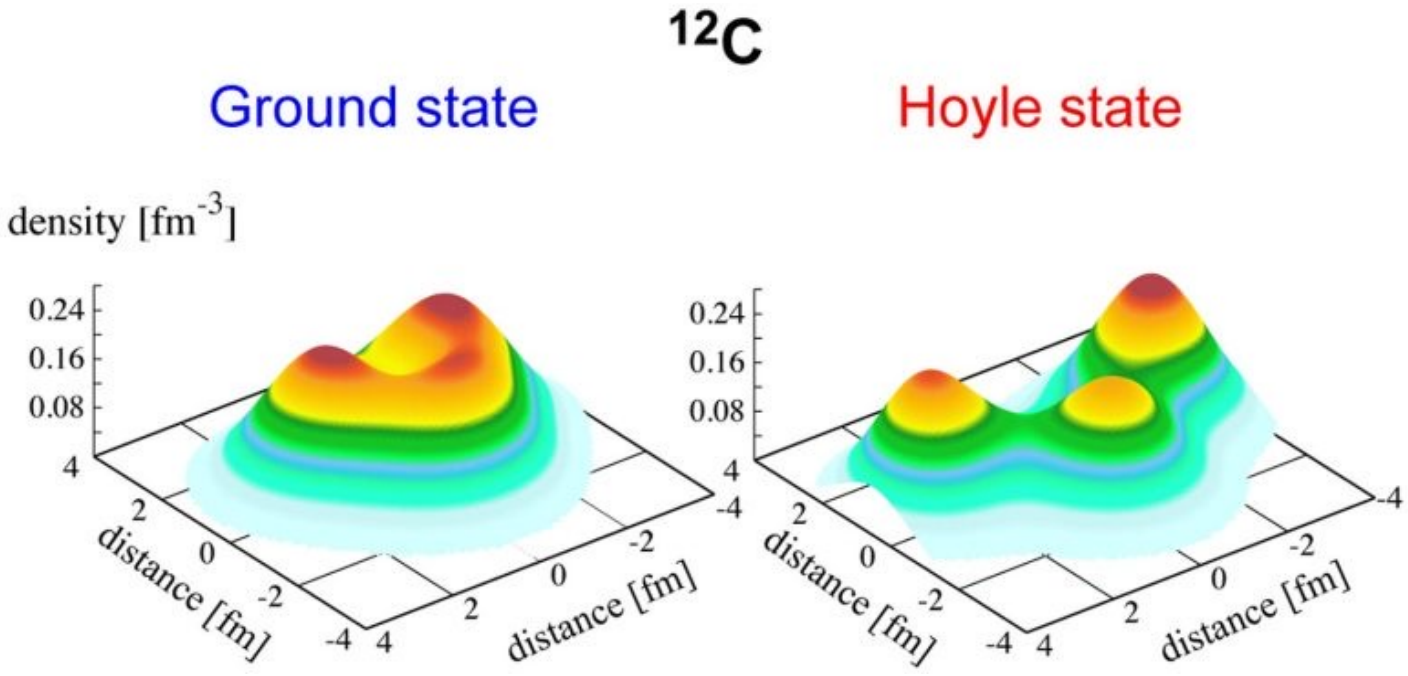

Otsuka et al., Nature Commun. 13, 2234 (2022)

Otsuka, Wednesday, November 13

Other example: ^{24}Mg

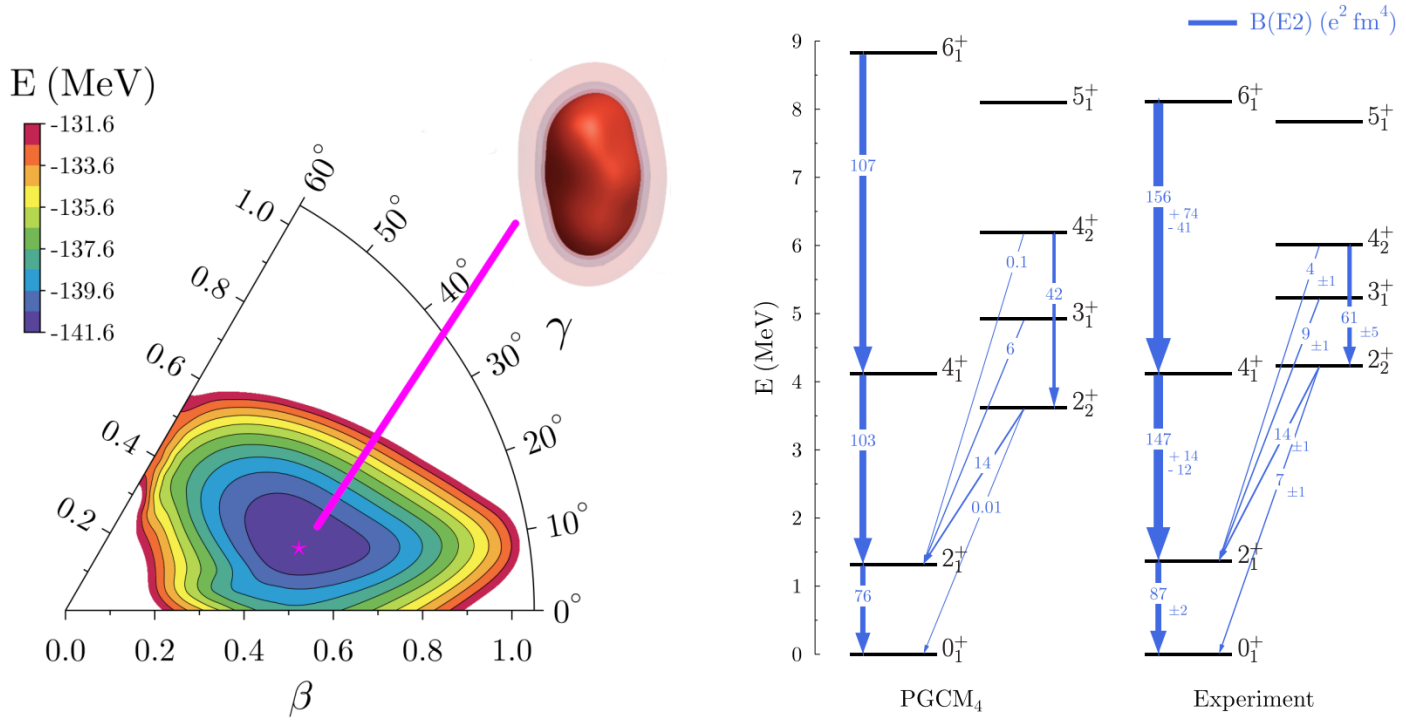

Bally, EPJA 60, 62 (2024)

- Ground state exhibits large intrinsic triaxial deformation
- Excellent description using χEFT Hamiltonian

Bally, Wednesday, November 13

Ab initio methods

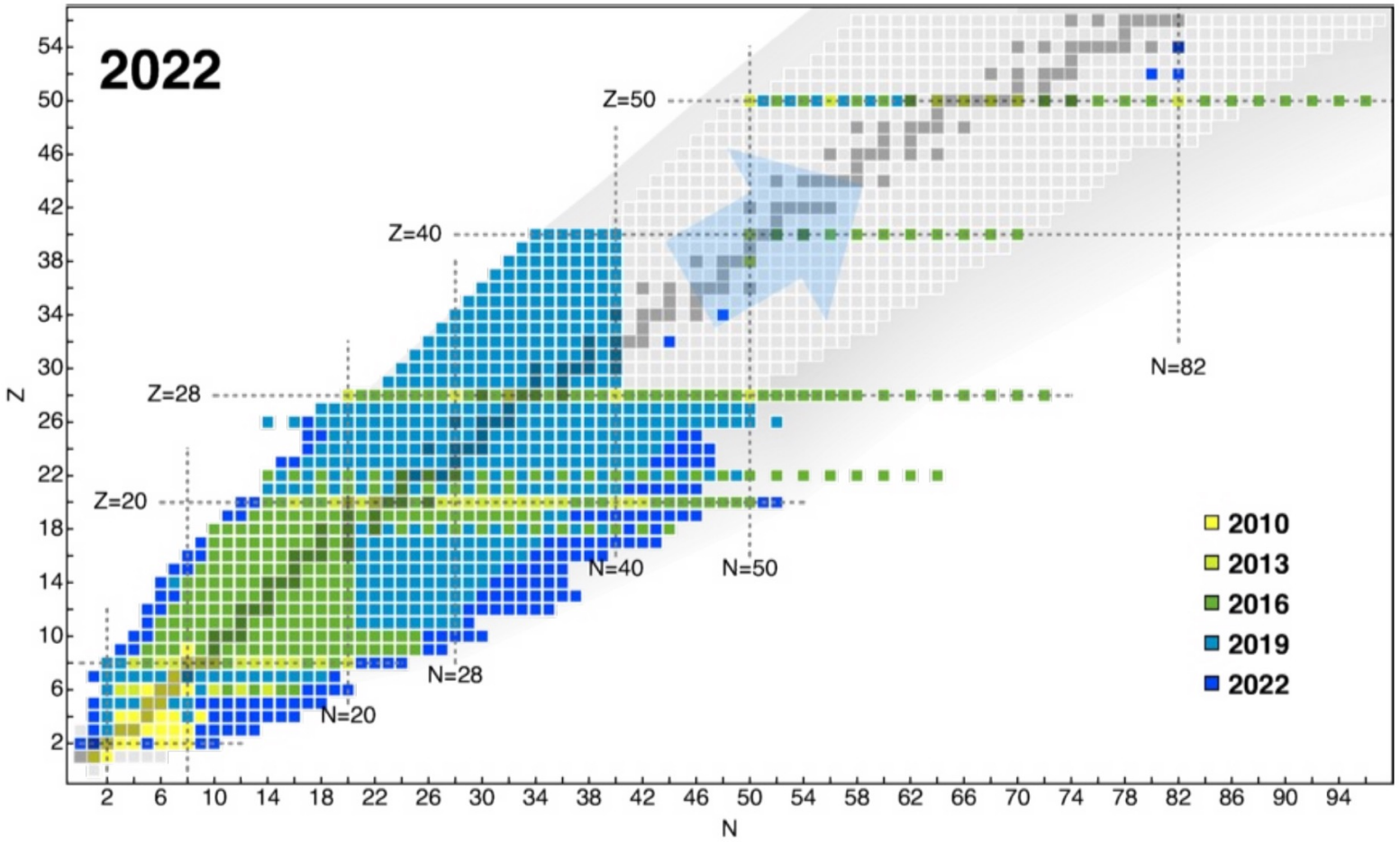

adapted from Hergert, Front. Phys. 8, 379 (2020)

Many-Body Perturbation Theory

Roth et al., Phys. Lett. B683, 272 (2010); Tichai et al., Phys. B756, 283 (2016)

$$|\Psi\rangle = |\Phi\rangle + \sum_{n=1}^{\infty} \left(\frac{1}{H_0 - E^{(0)}} H_I \right)^n |\Phi\rangle$$

$$E = E^{(0)} + \langle\Phi| \sum_{n=1}^{\infty} H_I \left(\frac{1}{H_0 - E^{(0)}} H_I \right)^n |\Phi\rangle$$

In-Medium Similarity Renormalization Group

Hergert et al., Phys. Rev. 621, 165 (2016); Stroberg et al., Phys. Rev. Lett. 118, 032502 (2017)

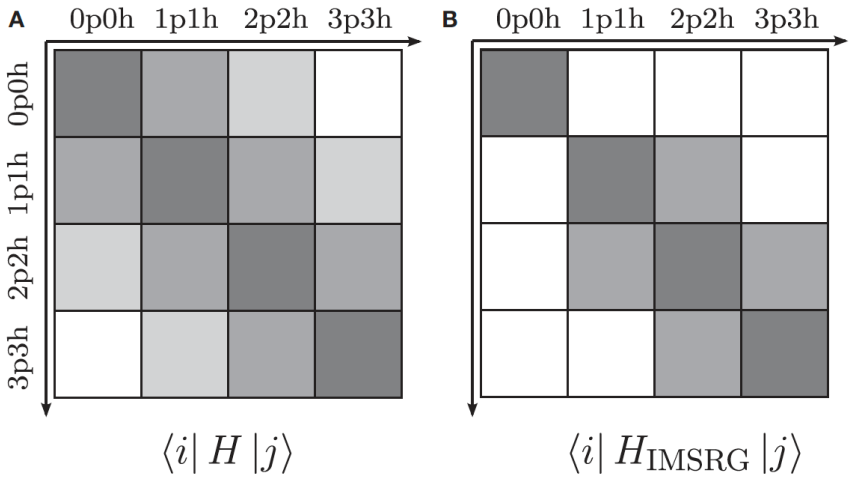

Hergert, Front. Phys. 8, 379 (2020)

Coupled Cluster Methods

Hagen et al., Rept. Prog. Phys. 77, 096302 (2014); Duguet et al., Phys. Rev. C 91, 064320 (2015)

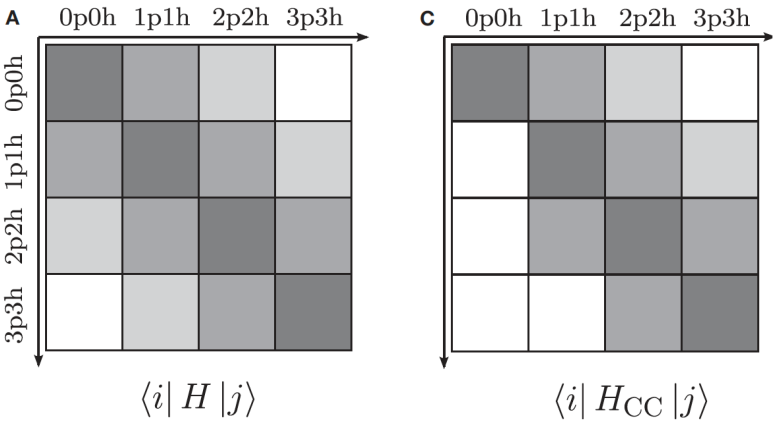

Self-Consistent Green's Functions

Dickhoff et al., Prog. Part. Nucl. Phys. 52, 377 (2004), Soma et al. Phys. Rev. C 101, 014318 (2020)

$$g_{pq\cdots rs} = \langle \Psi_0^A |\, T\left[a_p(t_p)a_q(t_q)\cdots a_s^\dagger(t_s)a_r^\dagger(t_r)\right] |\Psi_0^A\rangle$$

No-Core Configuration Interaction

Barrett et al., Prog. Part. Nucl. Phys. 69, 131 (2013); Navratil et al., Phys. Scripta. 91 053002, (2016)

$$|\Psi\rangle = |\Psi\rangle_{\text{core}} \otimes |\Psi\rangle_{\text{valence}} \rightarrow |\Psi\rangle_{\text{all valence}}$$

Symmetry-Adapted No-Core Configuration Interaction

Launey et al., Prog. Part. Nucl. Phys. 89, 101 (2016); Dytrych et al. Phys. Rev. Lett. 124, 042501 (2020)

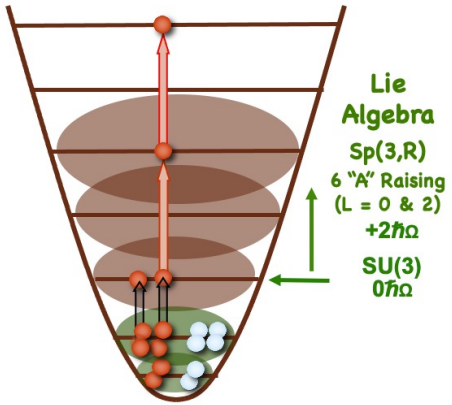

Quantum Monte Carlo

Carlson et al., Rev. Mod. Phys. 87, 1067 (2015); Gandolfi et al, Front. Phys. 8, 117 (2020)

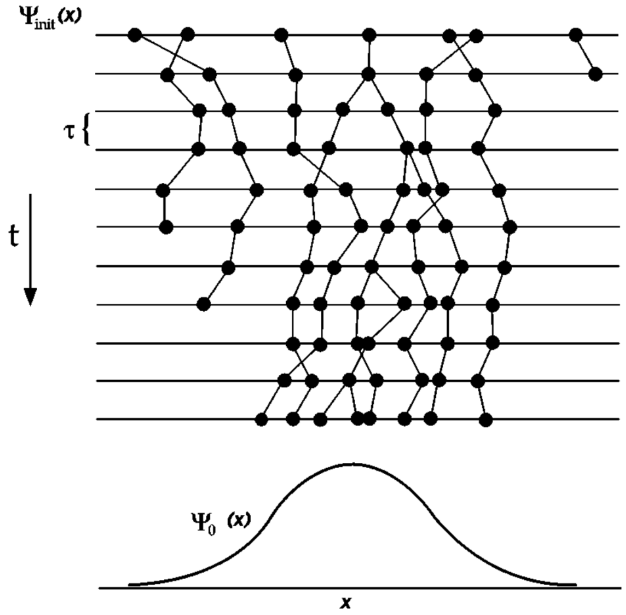

Foulkes et al., Rev. Mod. Phys. 73, 1 (2001)

Ab Initio Projected Variational Methods:

No-Core Monte Carlo Shell Model

Monte Carlo simulations used to optimize reference states

Otsuka et al., Prog. Part. Nucl. Phys. 47, 319 (2001); Shimizu, Phys. Scripta. 92, 063001 (2017)

Projected Generator Coordinate Method (PGCM)

Symmetry-breaking mean-field reference states

Frosini et al., Eur. Phys. J A 58, 63 (2022), Frosini et al., Eur. Phys. J A 58, 64 (2022)

$$|\Phi_i(J,M,\pi)\rangle = \sum_{K=-J}^{J} g_K P^J_{M,K} P^\pi |\phi_i\rangle$$

$$|\Psi(J,M,\pi)\rangle = \sum_{i=1}^{N_{\text{basis}}} f_i |\Phi_i(J,M,\pi)\rangle$$

Nuclear lattice effective field theory (NLEFT)

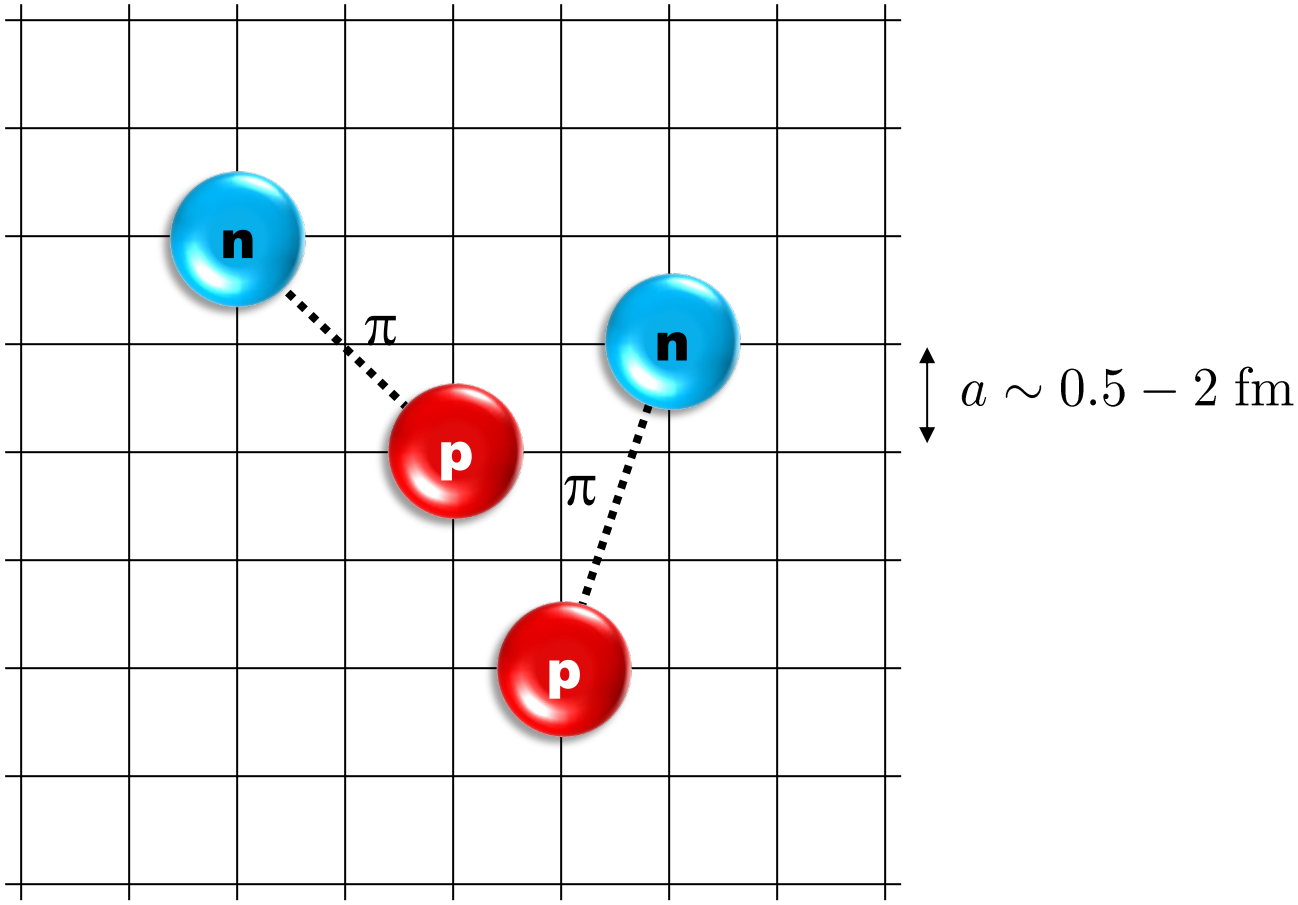

D.L, Prog. Part. Nucl. Phys. 63 117-154 (2009)

Lähde, Meißner, Nuclear Lattice Effective Field Theory (2019), Springer

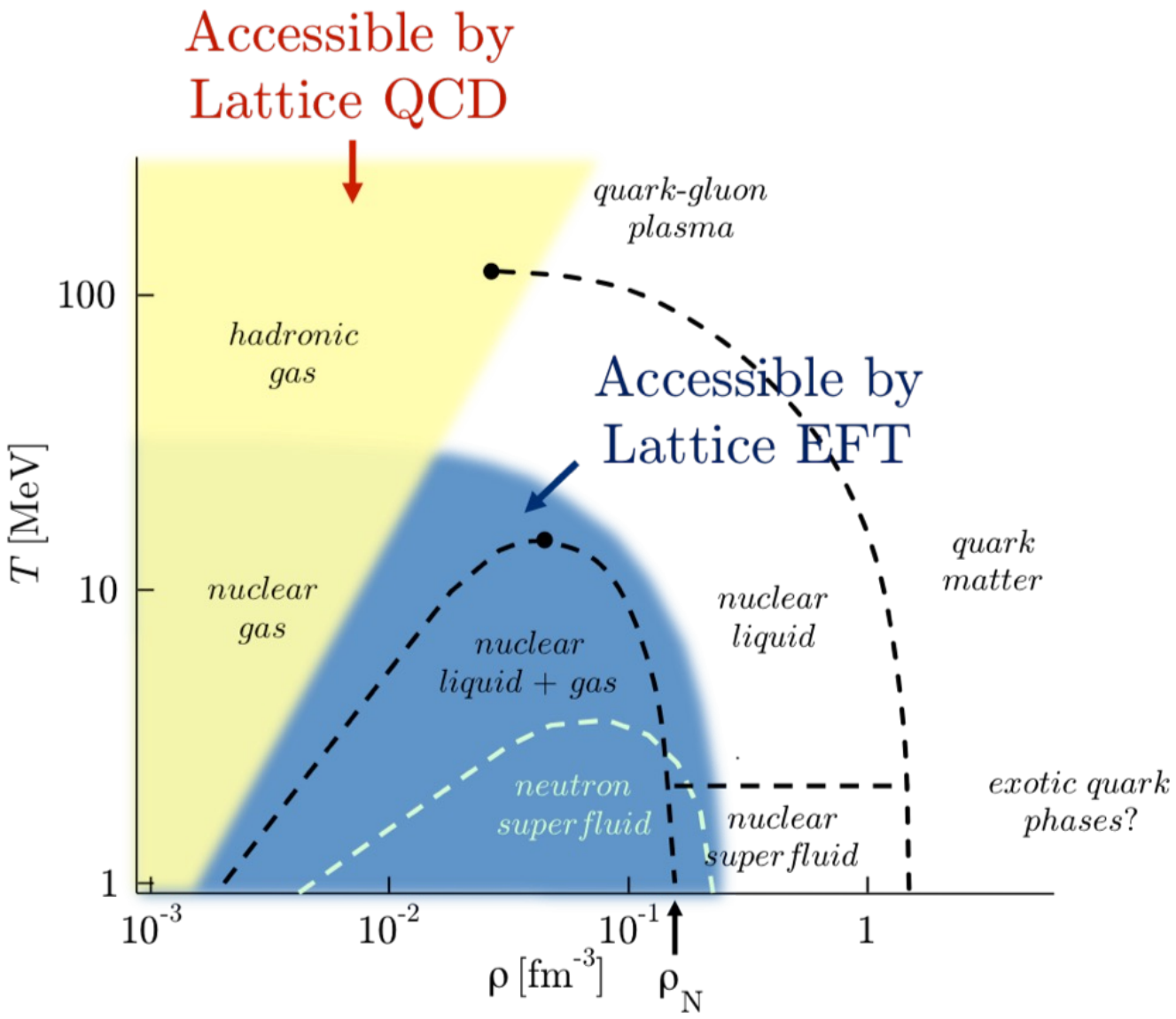
Accessible by
Lattice QCD
quark-gluon
plasma
hadronic
gas
Accessible by
Lattice EFT
quark
matter
nuclear
gas
nuclear
liquid
nuclear
liquid + gas
neutron
superfluid
nuclear
superfluid
exotic quark
phases?
100
10
1
T [MeV]
10^-3
10^-2
10^-1
1
ρ [fm^-3]
ρ_N

Chiral effective field theory

Construct the effective potential order by order

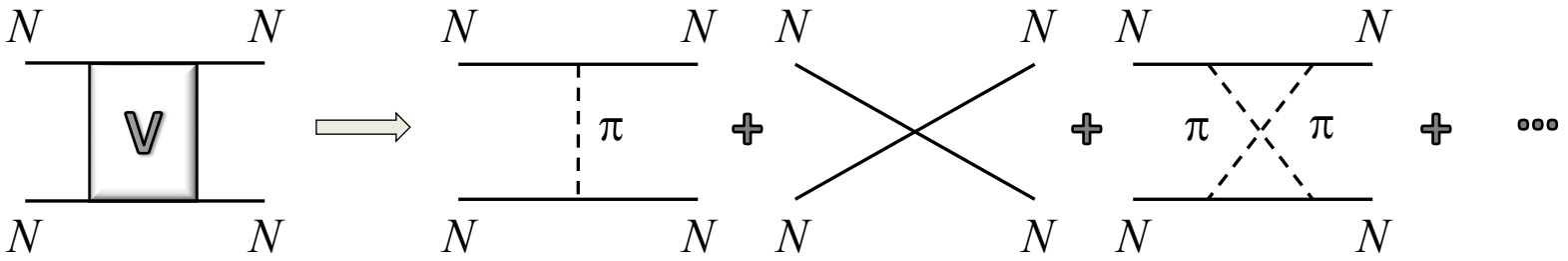

$V^{\rm OPEP}$ Contact interactions $V^{\rm TPEP}$

Leading order (LO) Next-to-leading order (NLO)

$a = 1.315\,\mathrm{fm}$

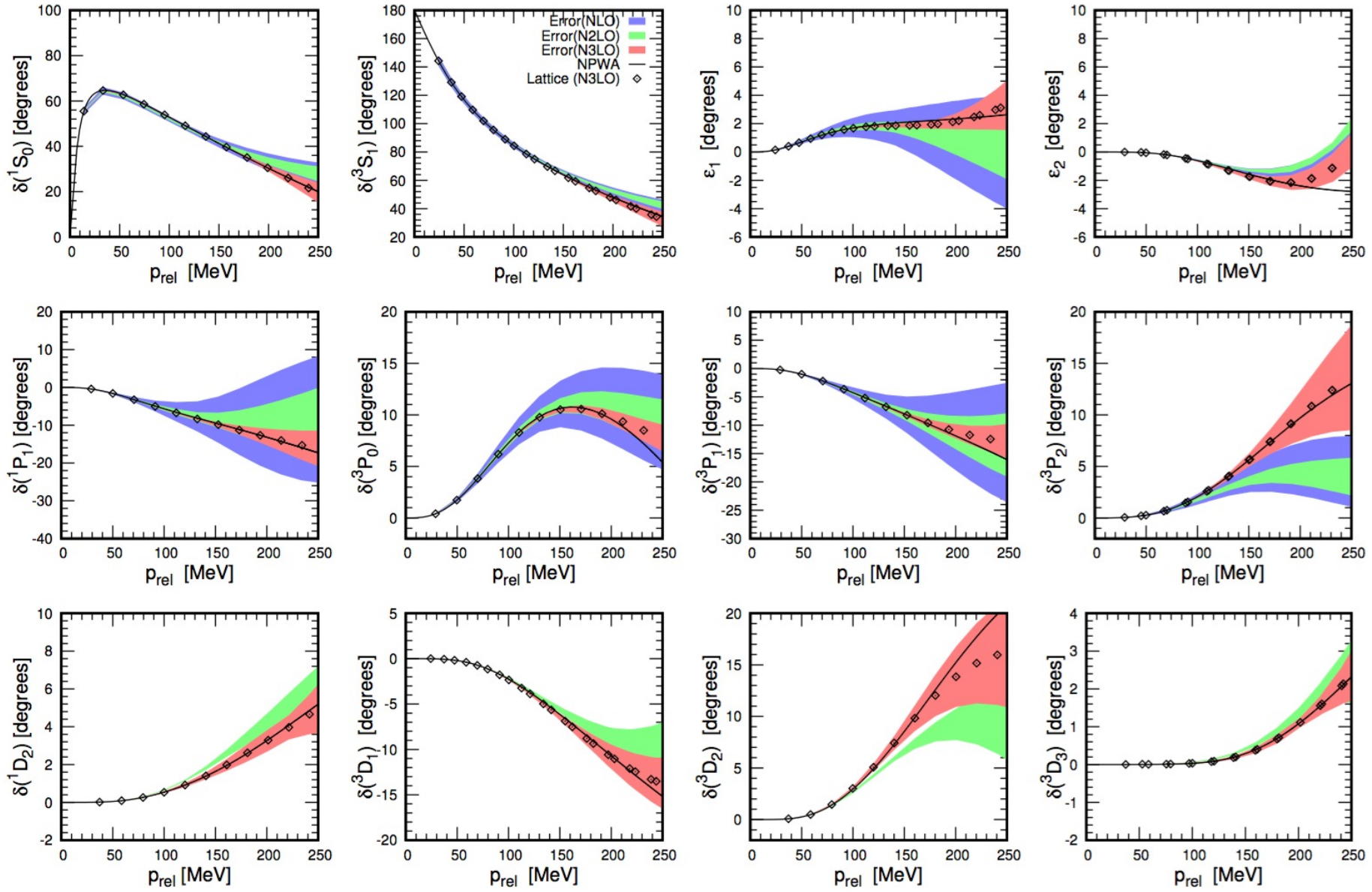

Li, Elhatisari, Epelbaum, D.L., Lu, Meißner, PRC 98, 044002 (2018)

$a = 0.987\,\mathrm{fm}$

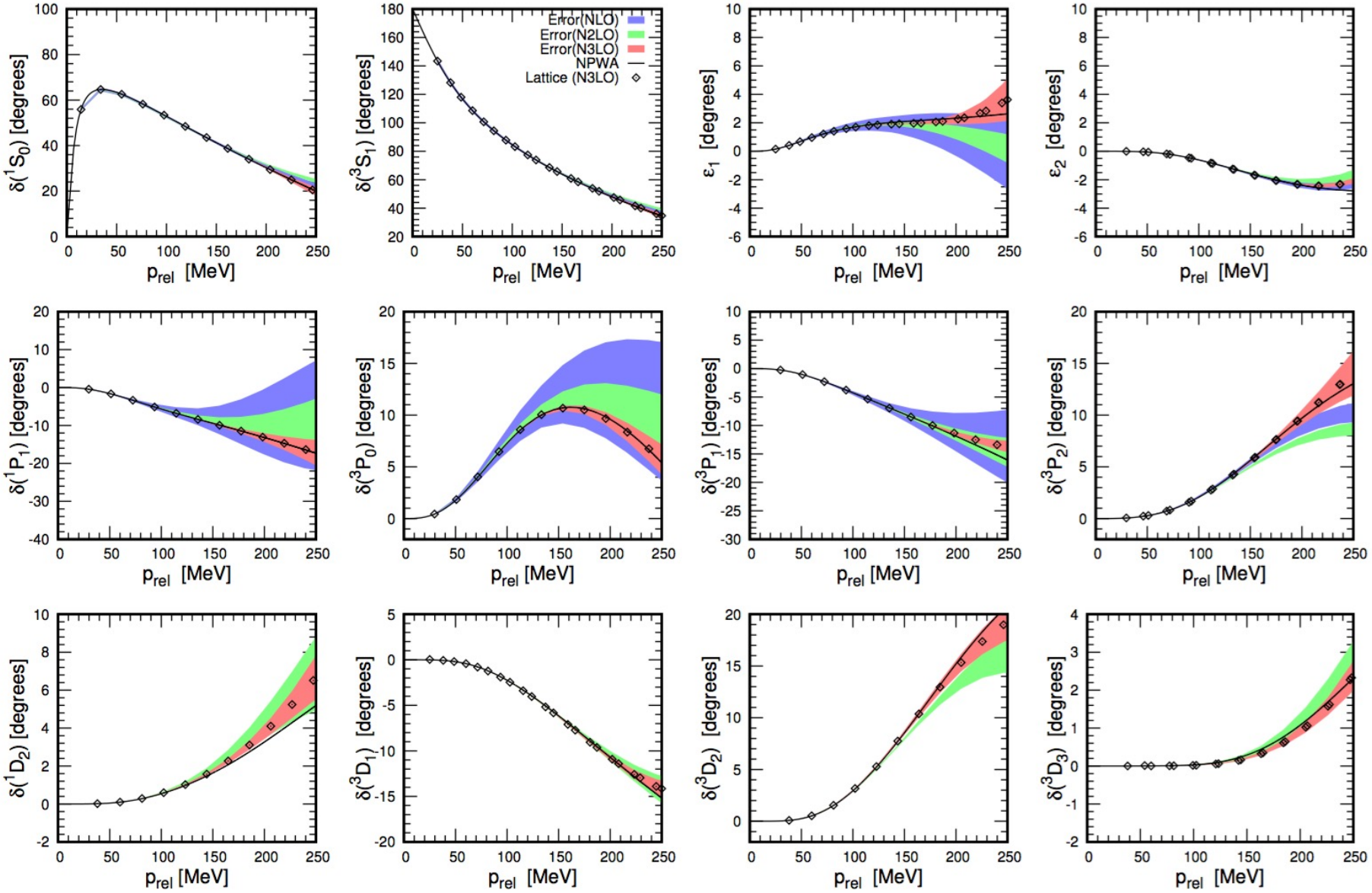

Euclidean time projection

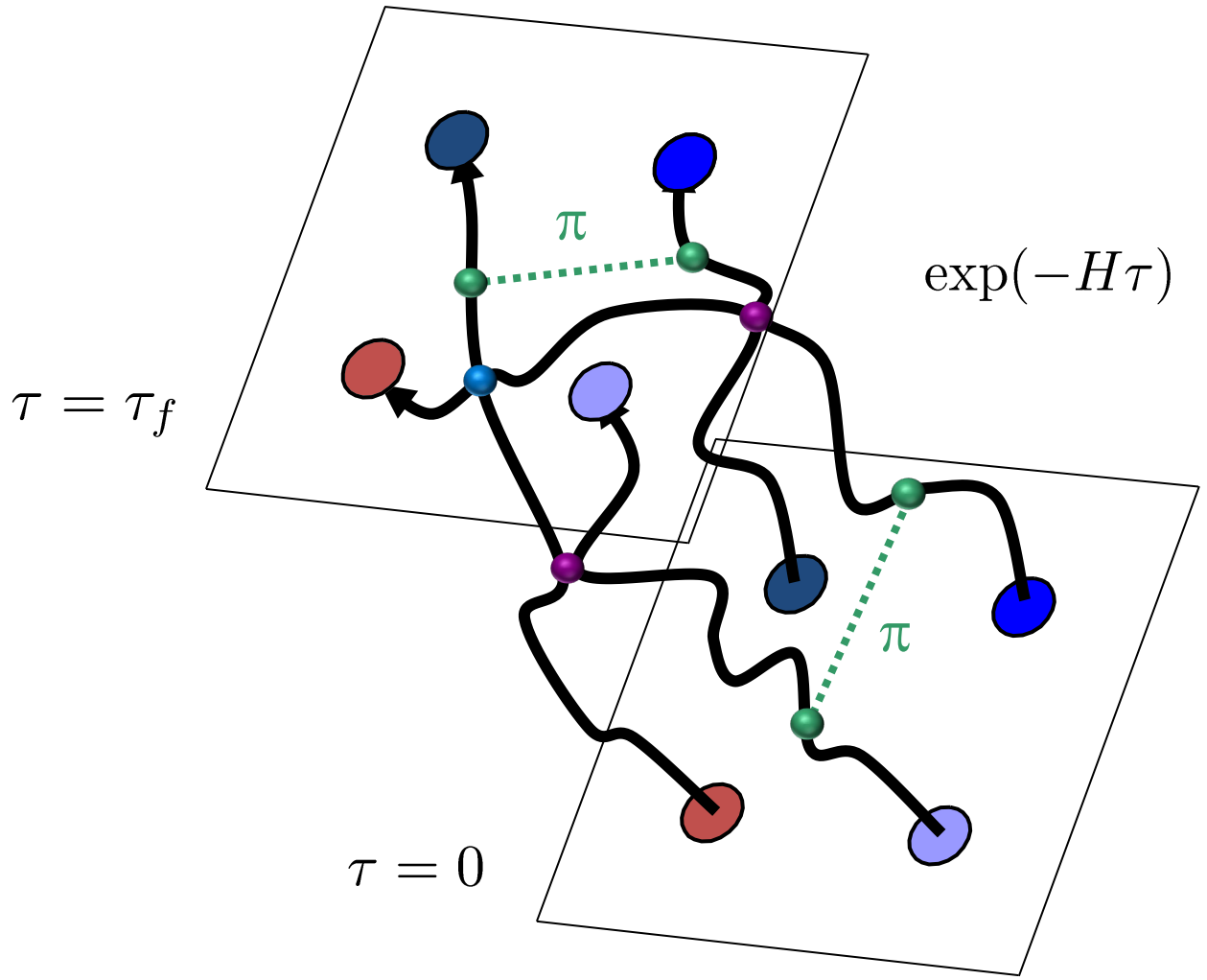

Auxiliary field method

We can write exponentials of the interaction using a Gaussian integral identity

$$\exp\left[-\frac{C}{2}(N^\dagger N)^2\right] \qquad \times \quad (N^\dagger N)^2$$

$$= \sqrt{\frac{1}{2\pi}}\int_{-\infty}^{\infty} ds \exp\left[-\frac{1}{2}s^2 + \sqrt{-C}\, s(N^\dagger N)\right] \qquad \rangle \bullet \; sN^\dagger N$$

We remove the interaction between nucleons and replace it with the interactions of each nucleon with a background field.

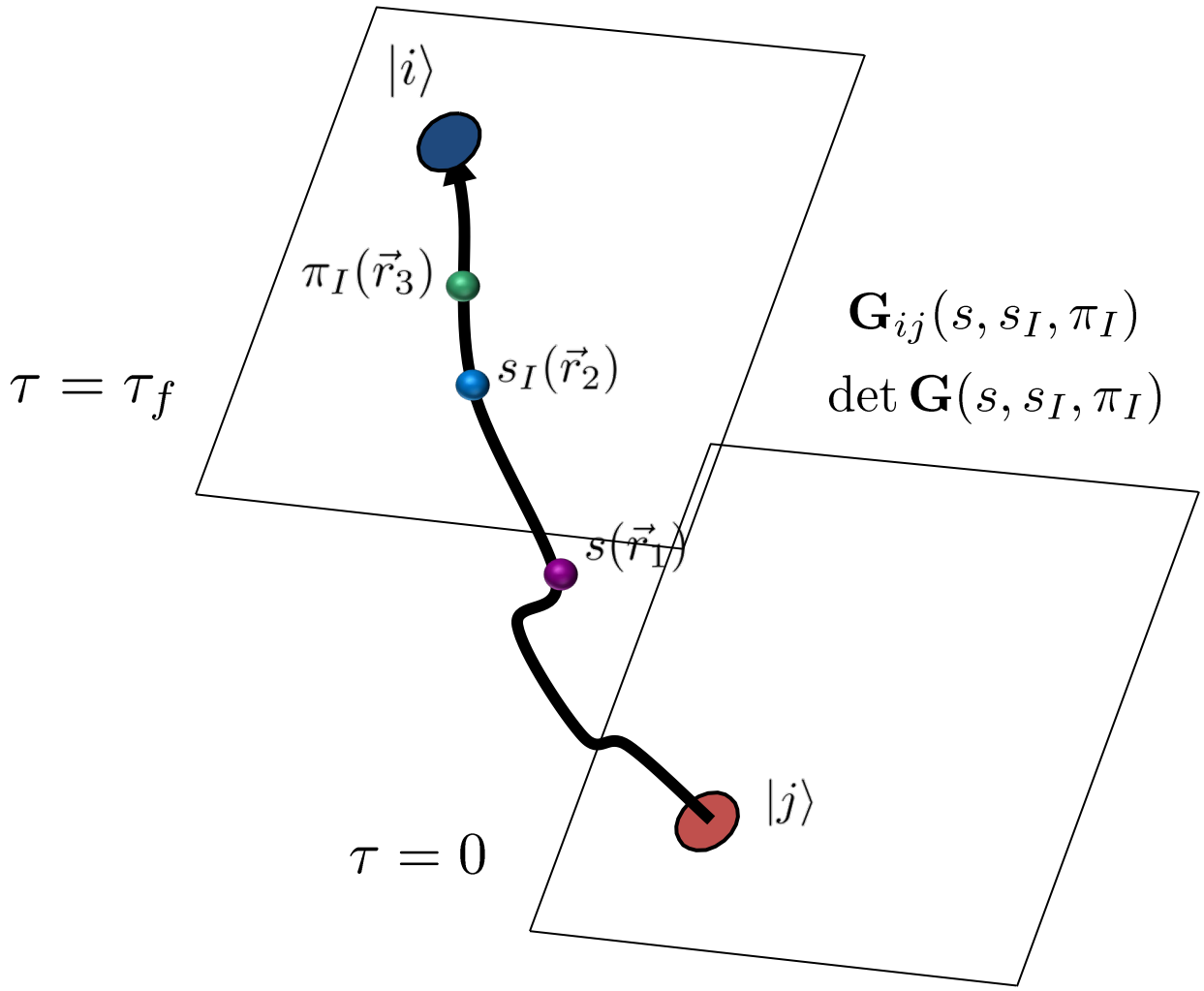
$|i\rangle$
$\pi_I(\vec{r}_3)$
$s_I(\vec{r}_2)$
$s(\vec{r}_1)$
$|j\rangle$
$\tau = \tau_f$
$\tau = 0$
$\mathbf{G}_{ij}(s, s_I, \pi_I)$
$\det \mathbf{G}(s, s_I, \pi_I)$

Essential elements for nuclear binding

What is the minimal nuclear interaction that can reproduce the ground state properties of light nuclei, medium-mass nuclei, and neutron matter simultaneously with no more than a few percent error in the energies and charge radii?

We construct an interaction with only four parameters.

1. Strength of the two-nucleon S-wave interaction
2. Range of the two-nucleon S-wave interaction
3. Strength of three-nucleon contact interaction

fit to $A = 2$, 3 systems

4. Range of the local part of the two-nucleon interaction

fit to A > 3

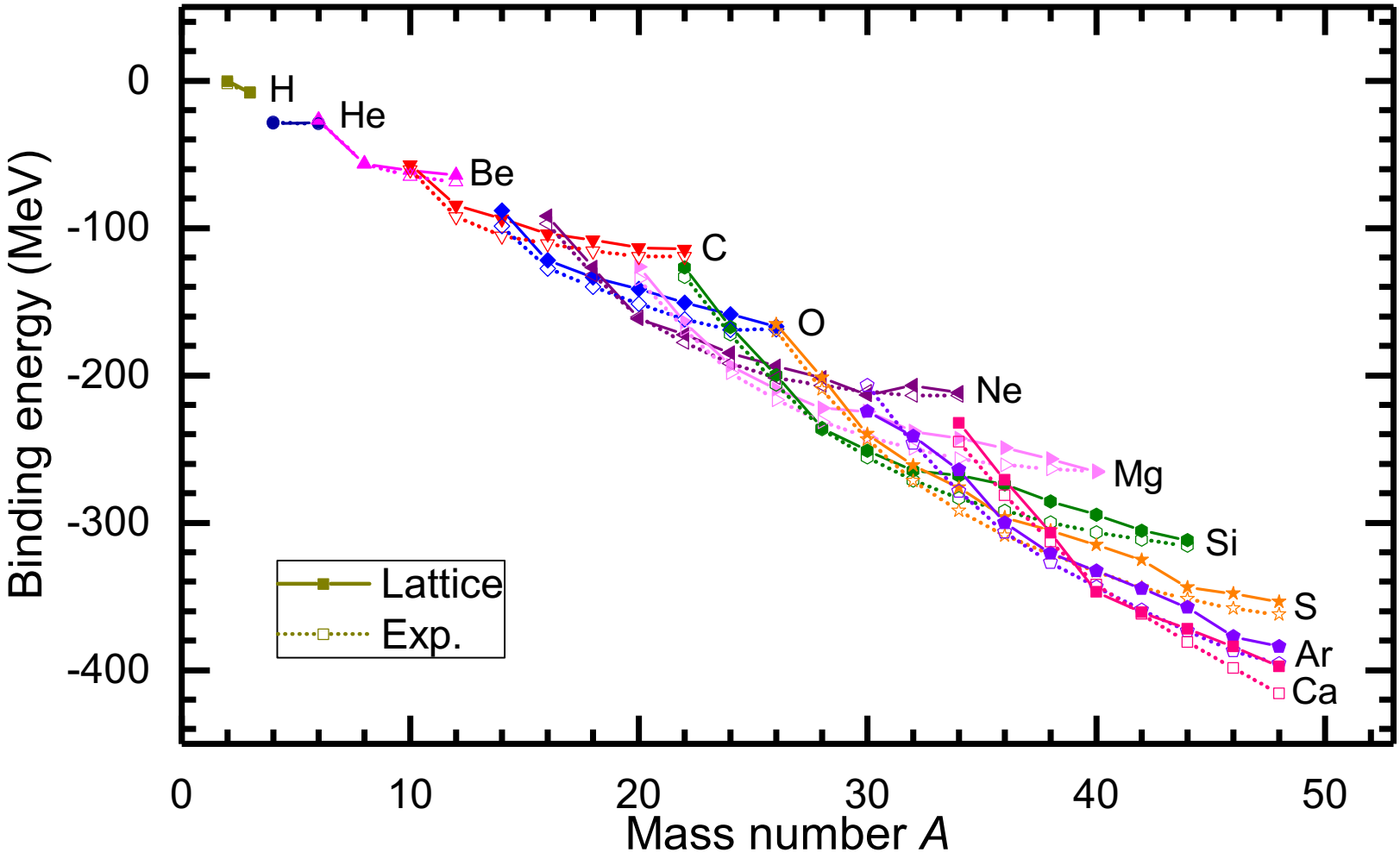

Lu, Li, Elhatisari, D.L., Epelbaum, Meißner, PLB 797, 134863 (2019)

	B	Exp.	$R_{\rm ch}$	Exp.
^{3}H	8.48(2)(0)	8.48	1.90(1)(1)	1.76
^{3}He	7.75(2)(0)	7.72	1.99(1)(1)	1.97
^{4}He	28.89(1)(1)	28.3	1.72(1)(3)	1.68
^{16}O	121.9(1)(3)	127.6	2.74(1)(1)	2.70
^{20}Ne	161.6(1)(1)	160.6	2.95(1)(1)	3.01
^{24}Mg	193.5(02)(17)	198.3	3.13(1)(2)	3.06
^{28}Si	235.8(04)(17)	236.5	3.26(1)(1)	3.12
^{40}Ca	346.8(6)(5)	342.1	3.42(1)(3)	3.48

Pinhole algorithm

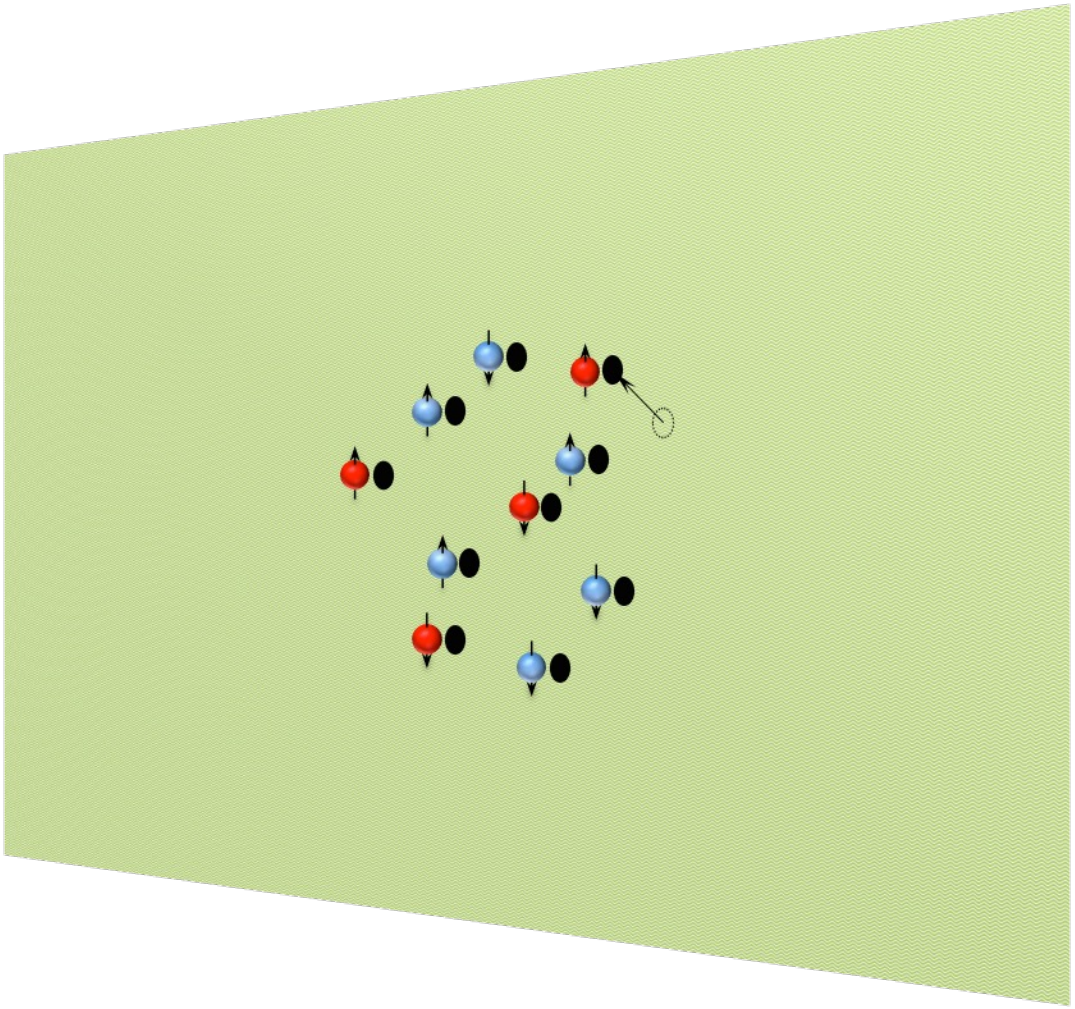

Seeing Structure with Pinholes

Consider the density operator for nucleon with spin i and isospin j

$$\rho_{i,j}(\mathbf{n}) = a^\dagger_{i,j}(\mathbf{n}) a_{i,j}(\mathbf{n})$$

We construct the normal-ordered A-body density operator

$$\rho_{i_1,j_1,\cdots i_A,j_A}(\mathbf{n}_1,\cdots \mathbf{n}_A) = :\rho_{i_1,j_1}(\mathbf{n}_1)\cdots\rho_{i_A,j_A}(\mathbf{n}_A):$$

In the simulations we do Monte Carlo sampling of the amplitude

$$A_{i_1,j_1,\cdots i_A,j_A}(\mathbf{n}_1,\cdots \mathbf{n}_A,t) = \langle\Psi_I|e^{-Ht/2}\rho_{i_1,j_1,\cdots i_A,j_A}(\mathbf{n}_1,\cdots \mathbf{n}_A)e^{-Ht/2}|\Psi_I\rangle$$

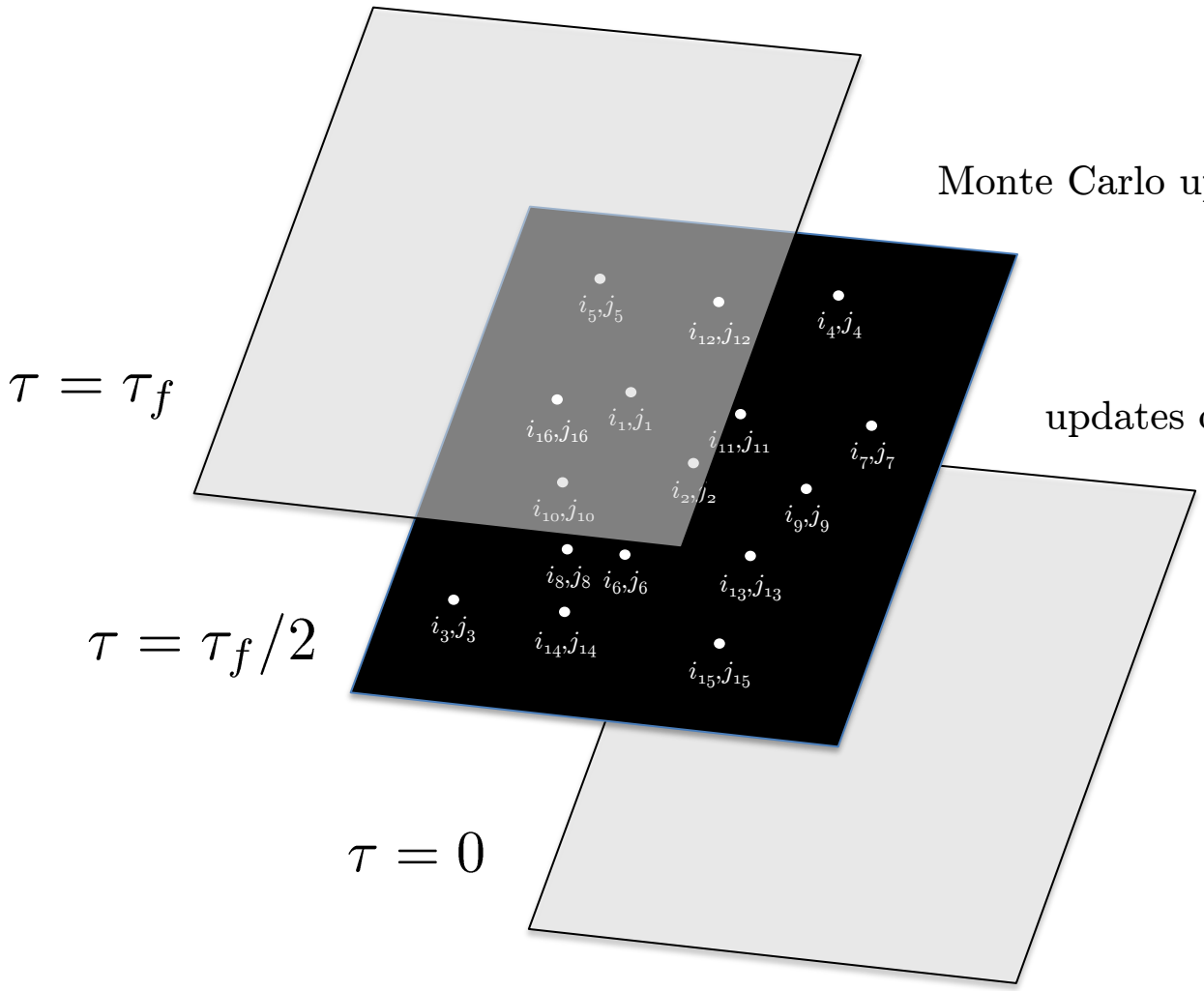

Monte Carlo updates of pinholes

Monte Carlo
updates of auxiliary/pion fields

Elhatisari, Epelbaum, Krebs, Lähde, D.L., Li, Lu, Meißner, Rupak, PRL 119, 222505 (2017)

Emergent geometry and duality of ^{12}C

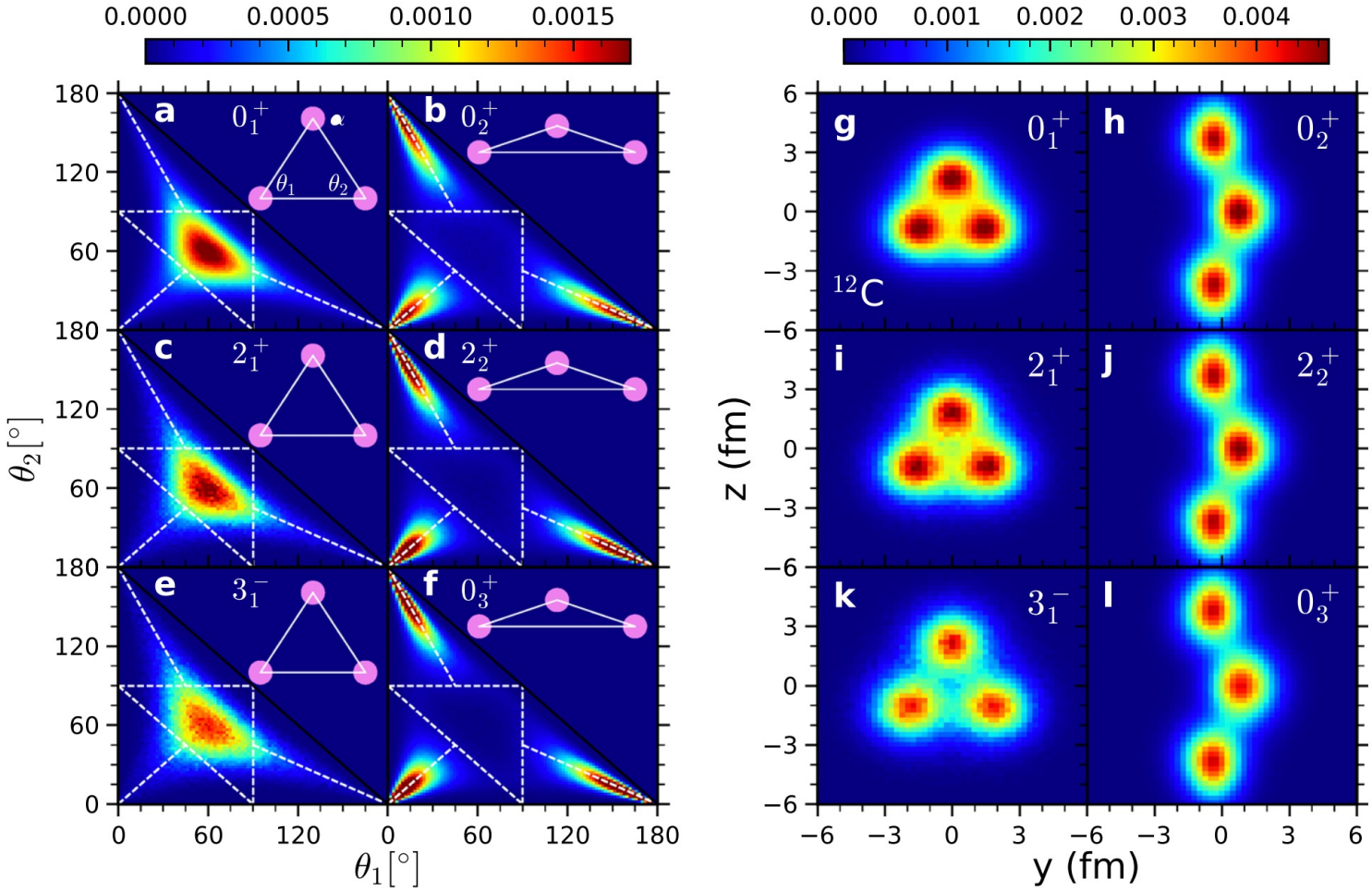

Shen, Elhatisari, Lähde, D.L., Lu, Meißner, Nature Commun. 14, 2777 (2023)

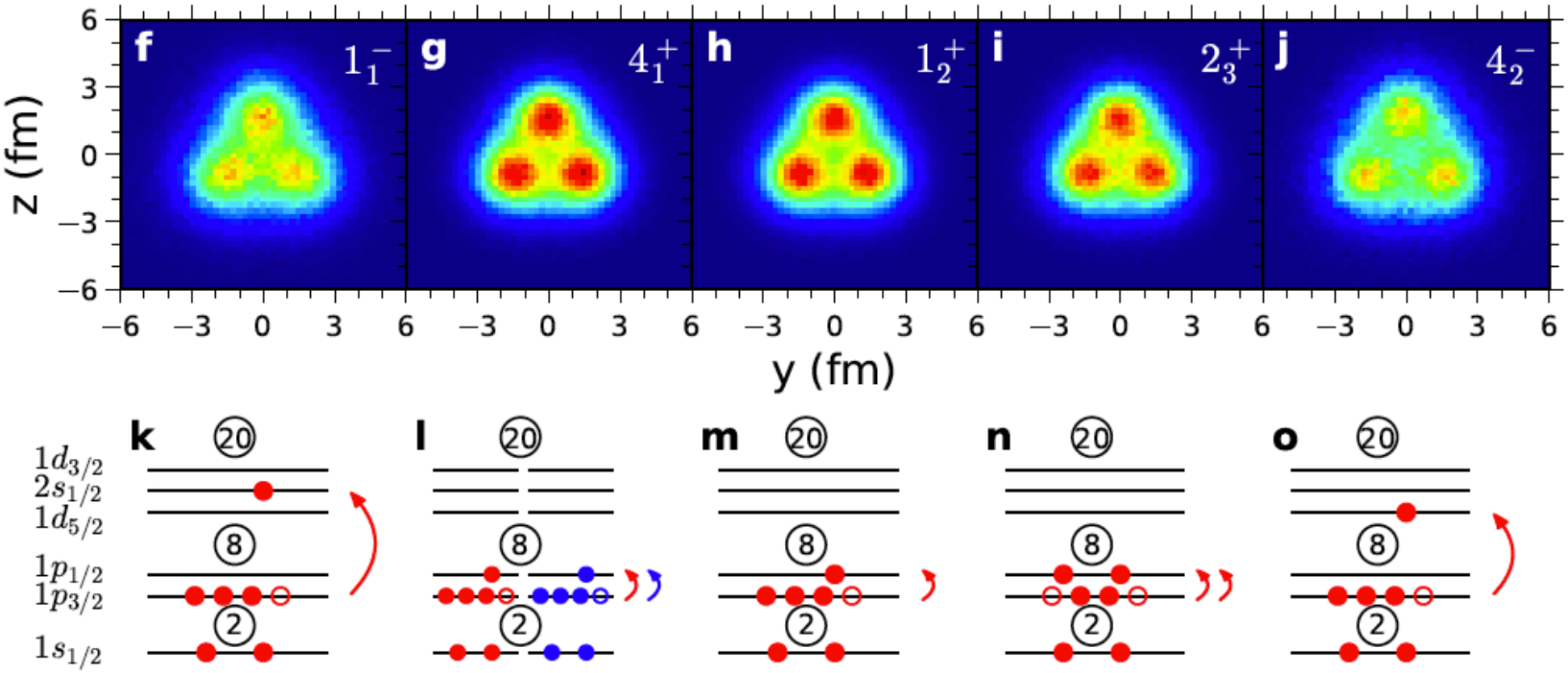
f
1^-_1
g
4^+_1
h
1^+_2
i
2^+_3
j
4^-_2
z (fm)
y (fm)
6
3
0
−3
−6
k
l
m
n
o
20
8
2
$1d_{3/2}$
$2s_{1/2}$
$1d_{5/2}$
$1p_{1/2}$
$1p_{3/2}$
$1s_{1/2}$

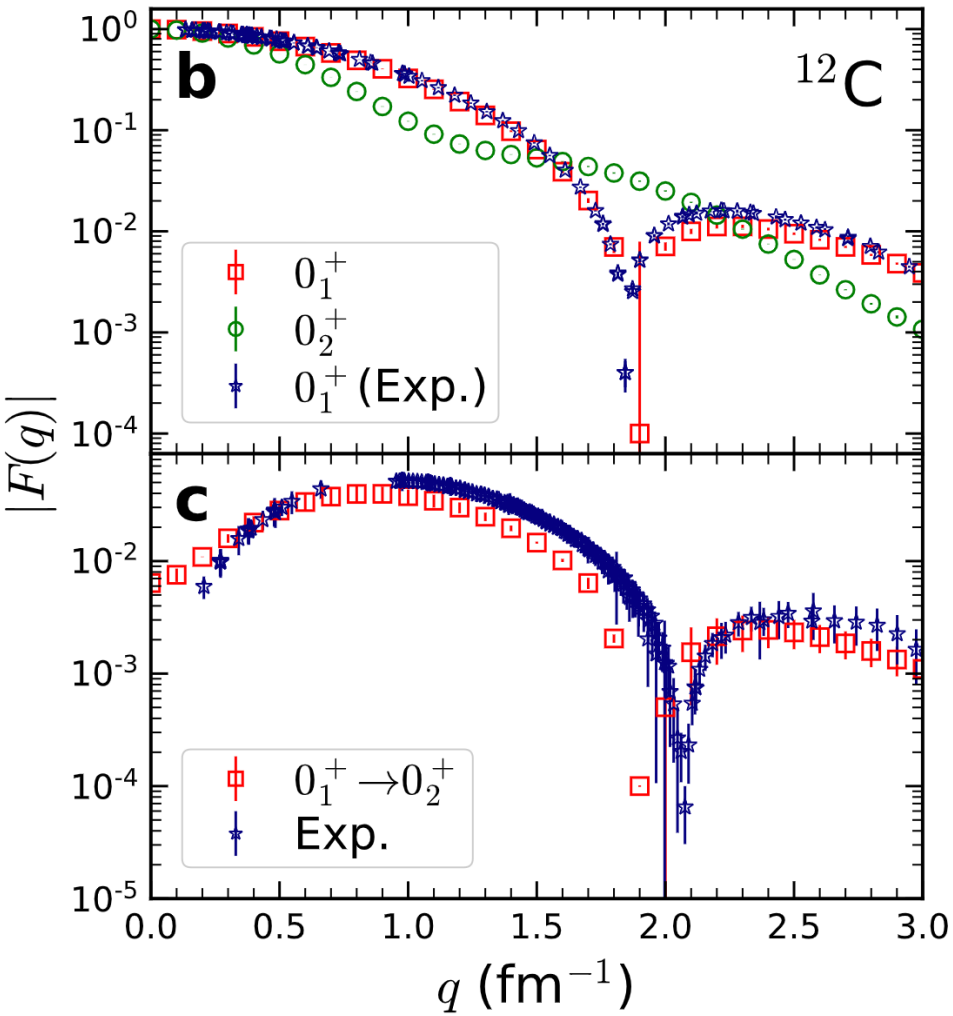

Shen, Elhatisari, Lähde, D.L., Lu, Meißner, Nature Commun. 14, 2777 (2023)

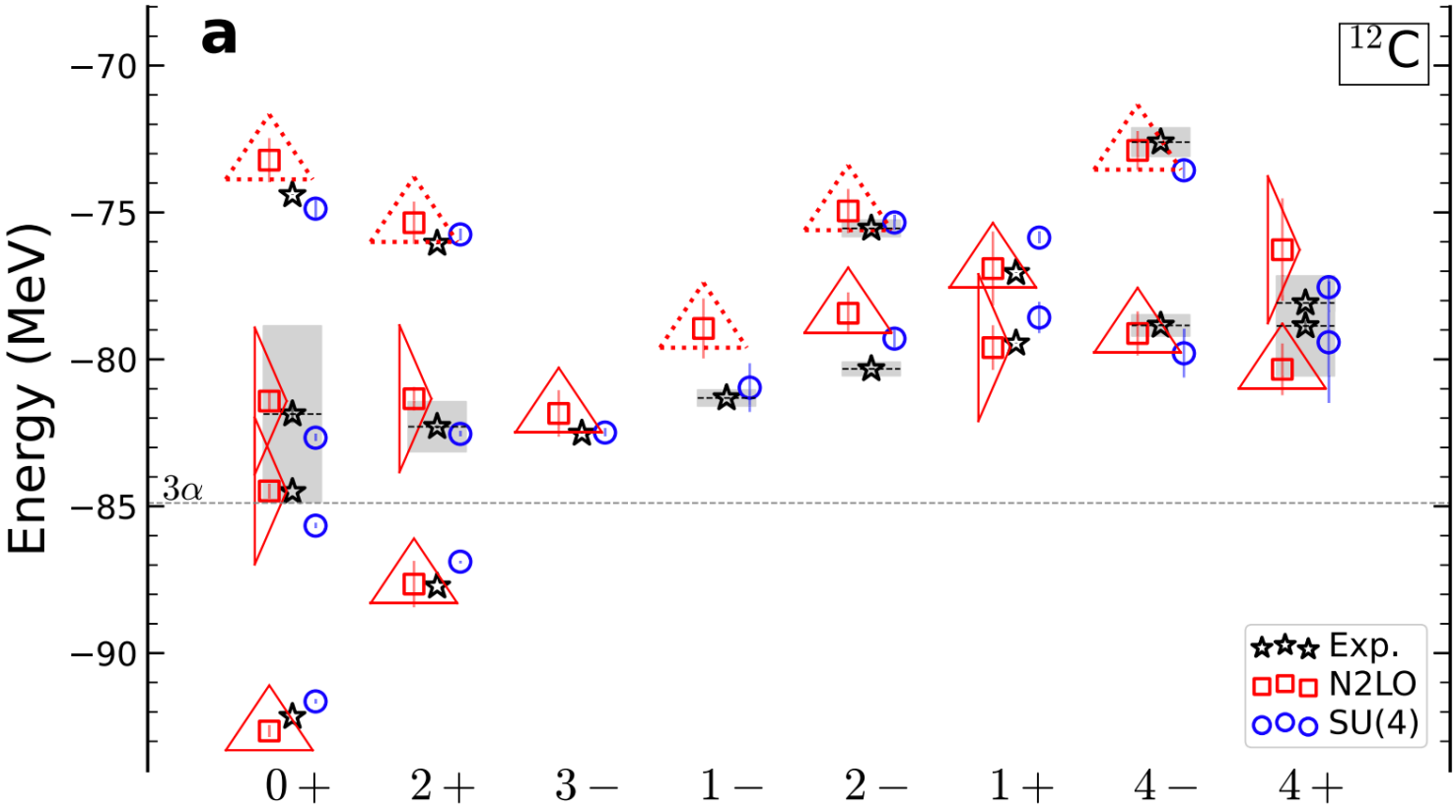

Shen, Elhatisari, Lähde, D.L., Lu, Meißner, Nature Commun. 14, 2777 (2023)

Recent advances using NLEFT

Ab initio nuclear thermodynamics

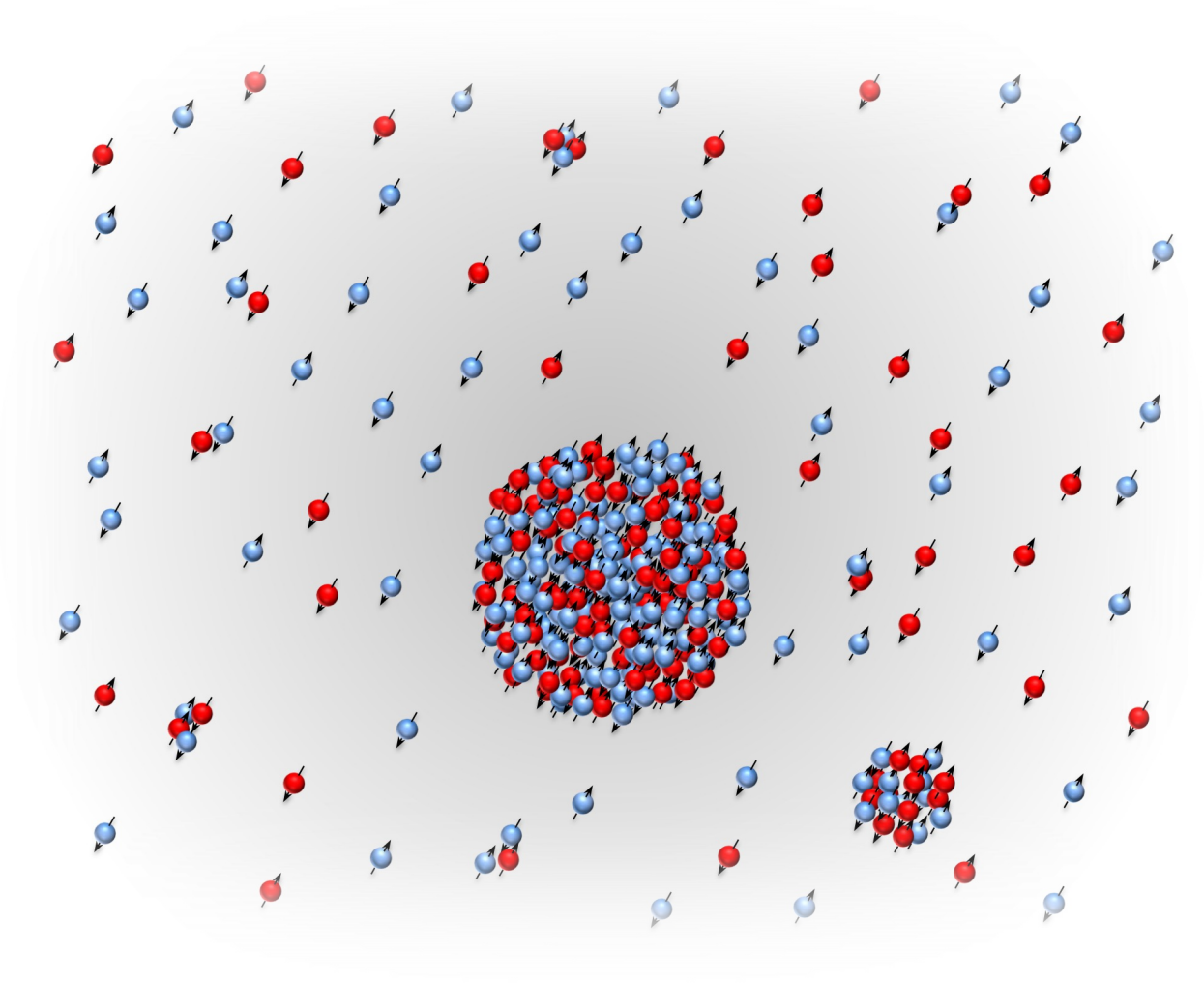

Lu, Li, Elhatisari, D.L., Drut, Lähde, Epelbaum, Meißner, Phys. Rev. Lett. 125, 192502 (2020)

Ab initio nuclear thermodynamics

In order to compute thermodynamic properties of finite nuclei, nuclear matter, and neutron matter, we need to compute the partition function

$$\mathrm{Tr}\exp(-\beta H)$$

We compute the quantum mechanical trace over A-nucleon states by summing over pinholes (position eigenstates) for the initial and final states

$$\mathrm{Tr}\, O = \frac{1}{A!} \sum_{i_1 \cdots i_A, j_1 \cdots j_A, \mathbf{n}_1 \cdots \mathbf{n}_A} \langle 0 | a_{i_A,j_A}(\mathbf{n}_A) \cdots a_{i_1,j_1}(\mathbf{n}_1)\, O\, a^\dagger_{i_1,j_1}(\mathbf{n}_1) \cdots a^\dagger_{i_A,j_A}(\mathbf{n}_A) | 0 \rangle$$

This can be used to calculate the partition function in the canonical ensemble.

Metropolis updates of pinholes

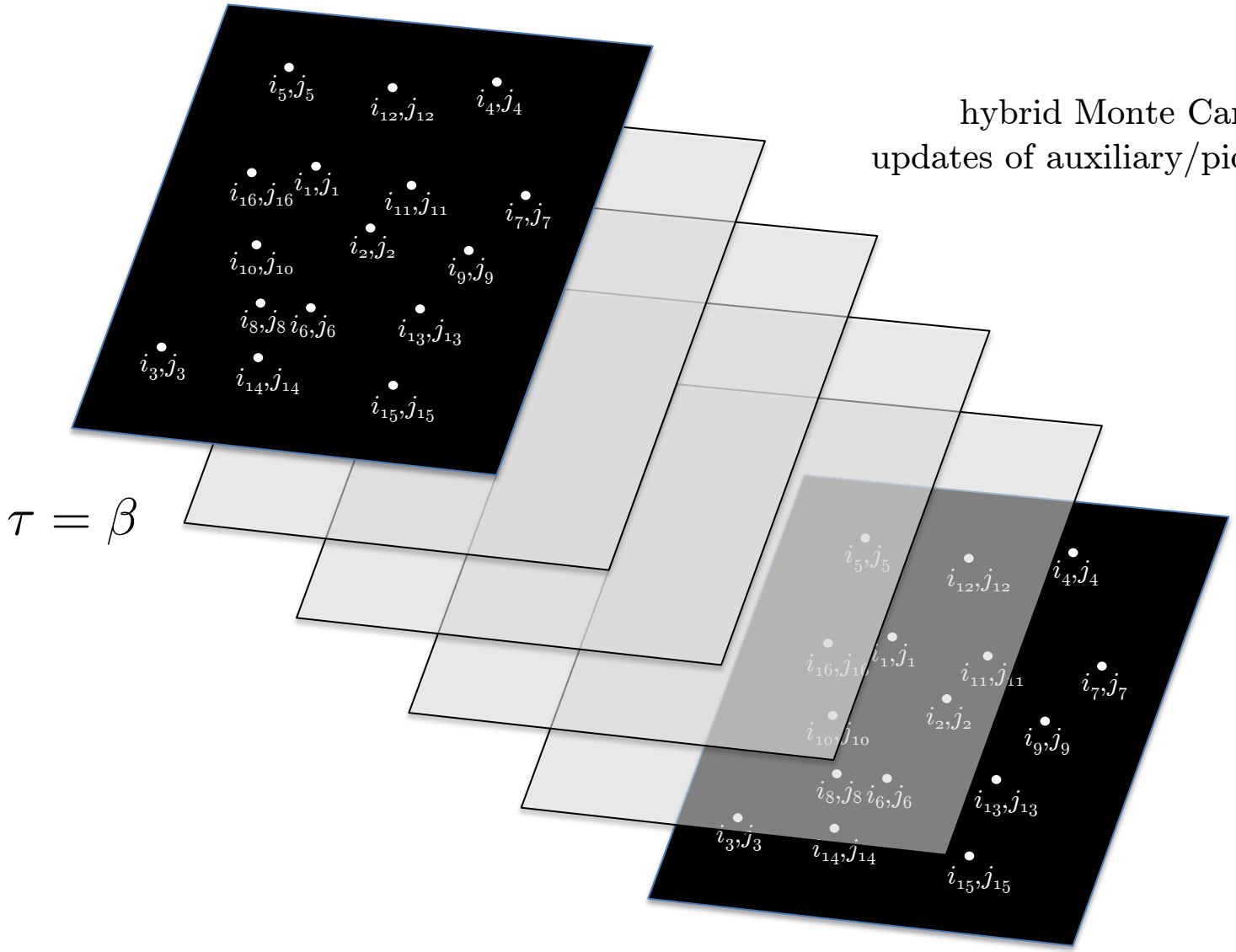

hybrid Monte Carlo
updates of auxiliary/pion fields

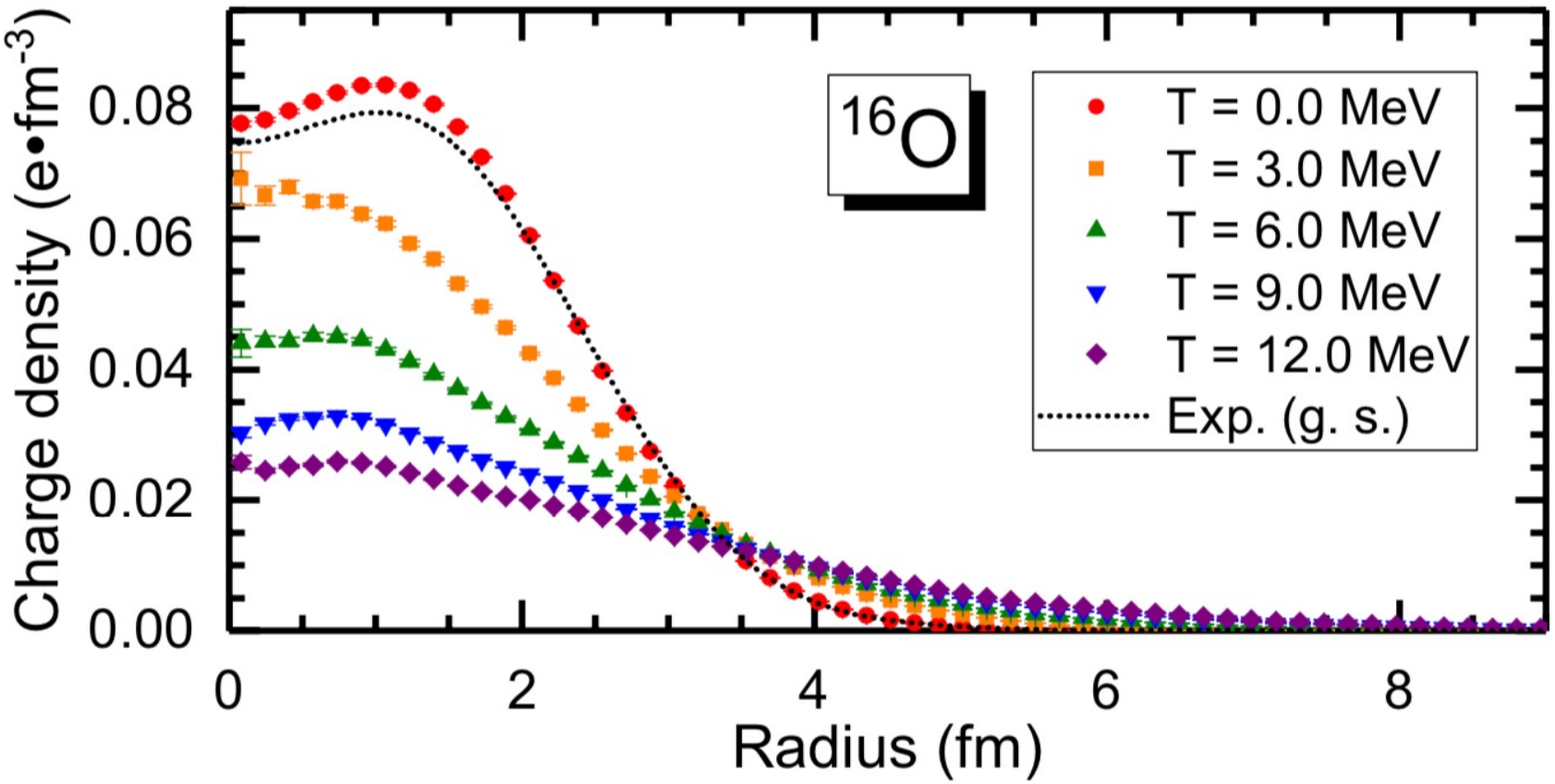
Charge density (e•fm^{-3})
0.00
0.02
0.04
0.06
0.08
0
2
4
6
8
Radius (fm)
^{16}O
T = 0.0 MeV
T = 3.0 MeV
T = 6.0 MeV
T = 9.0 MeV
T = 12.0 MeV
Exp. (g. s.)

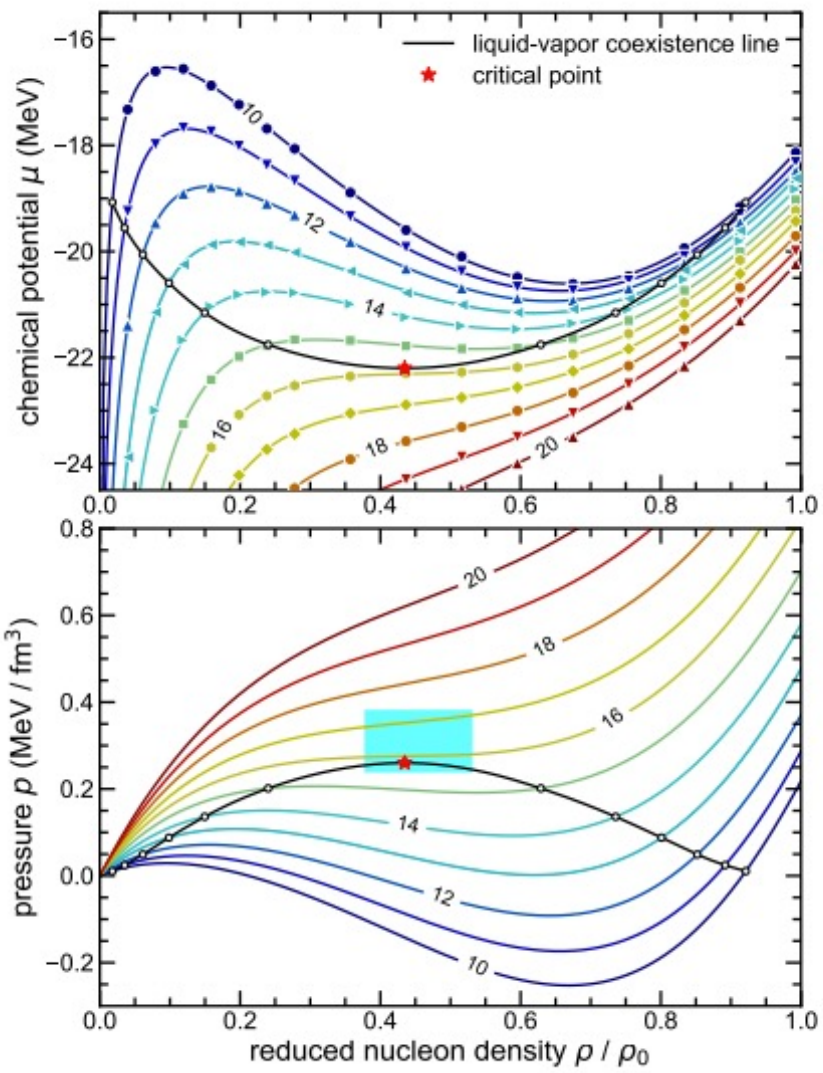

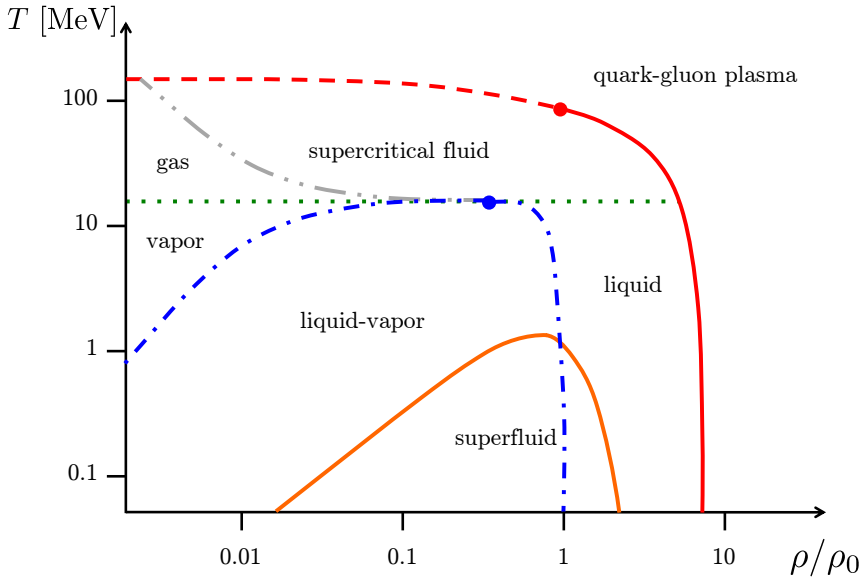

$$T_c = 15.80(0.32)(1.60)\,\mathrm{MeV}$$
$$\rho_c = 0.089(04)(18)\,\mathrm{fm}^{-3}$$
$$\mu_c = -22.20(0.44)(2.20)\,\mathrm{MeV}$$
$$P_c = 0.260(05)(30)\,\mathrm{MeV\ fm}^{-3}$$

Lu, Li, Elhatisari, D.L., Drut, Lähde, Epelbaum, Meißner, Phys. Rev. Lett. 125, 192502 (2020)

Wavefunction matching

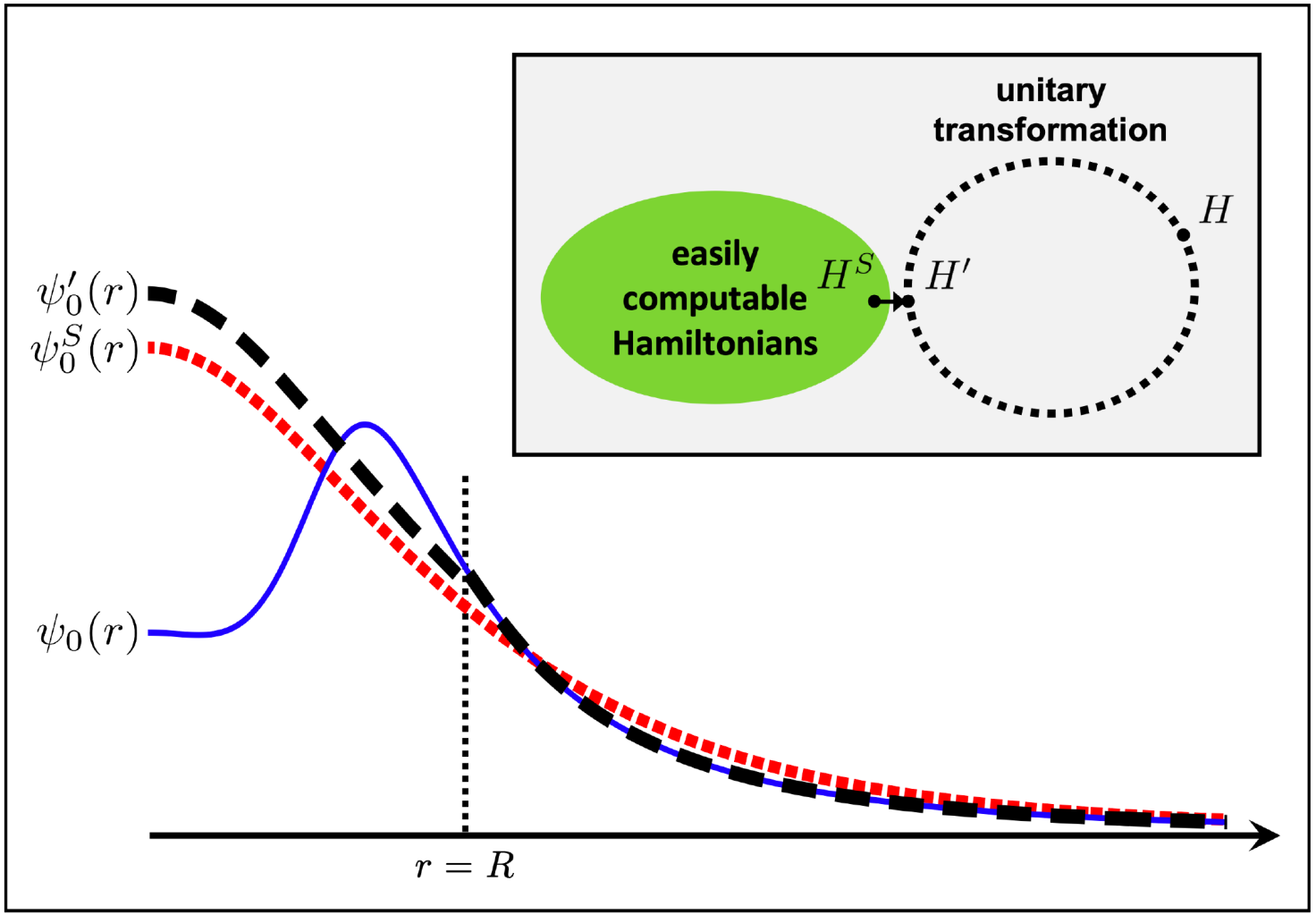

Elhatisari, Bovermann, Ma, Epelbaum, Frame, Hildenbrand, Krebs, Lähde, D.L., Li, Lu, M. Kim, Y. Kim, Meißner, Rupak, Shen, Song, Stellin, Nature 630, 59 (2024)

Ground state wavefunctions

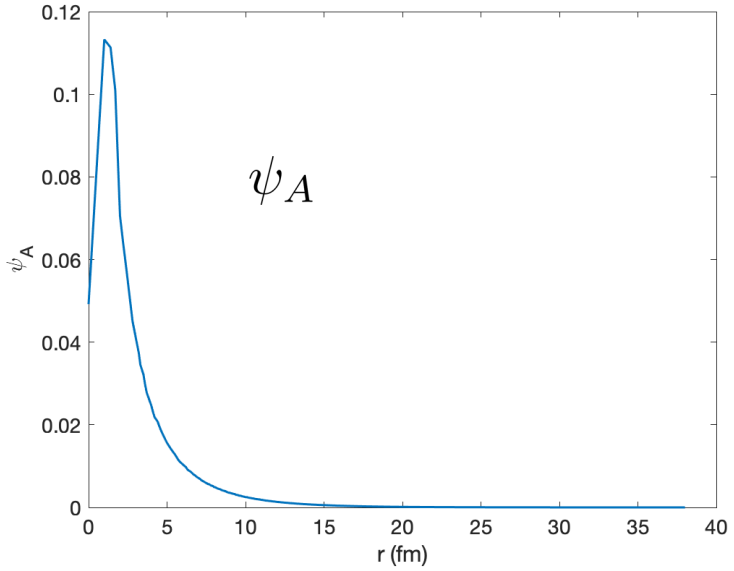

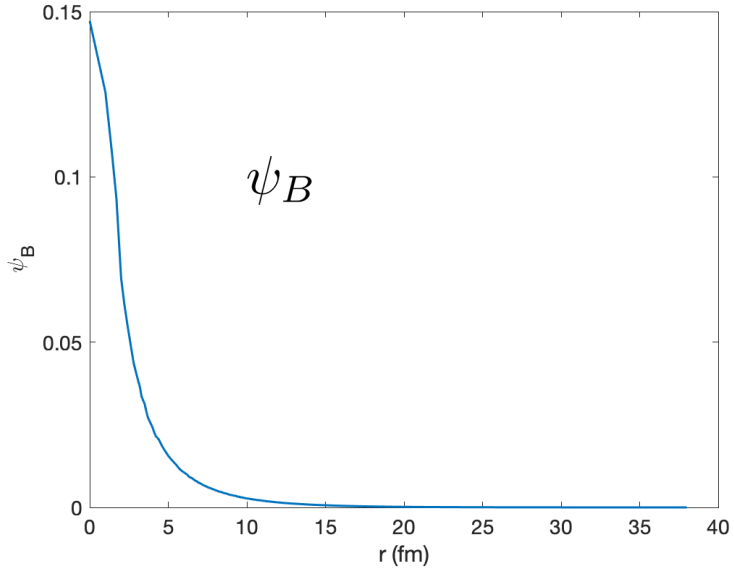

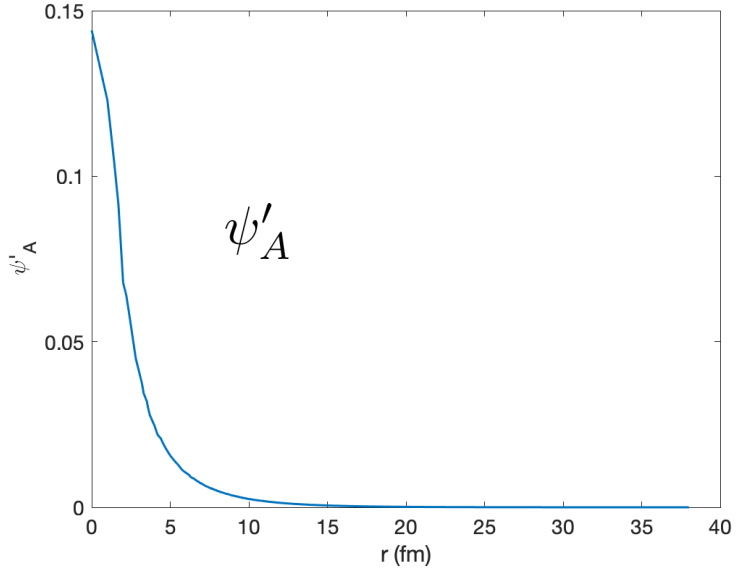

Binding energies

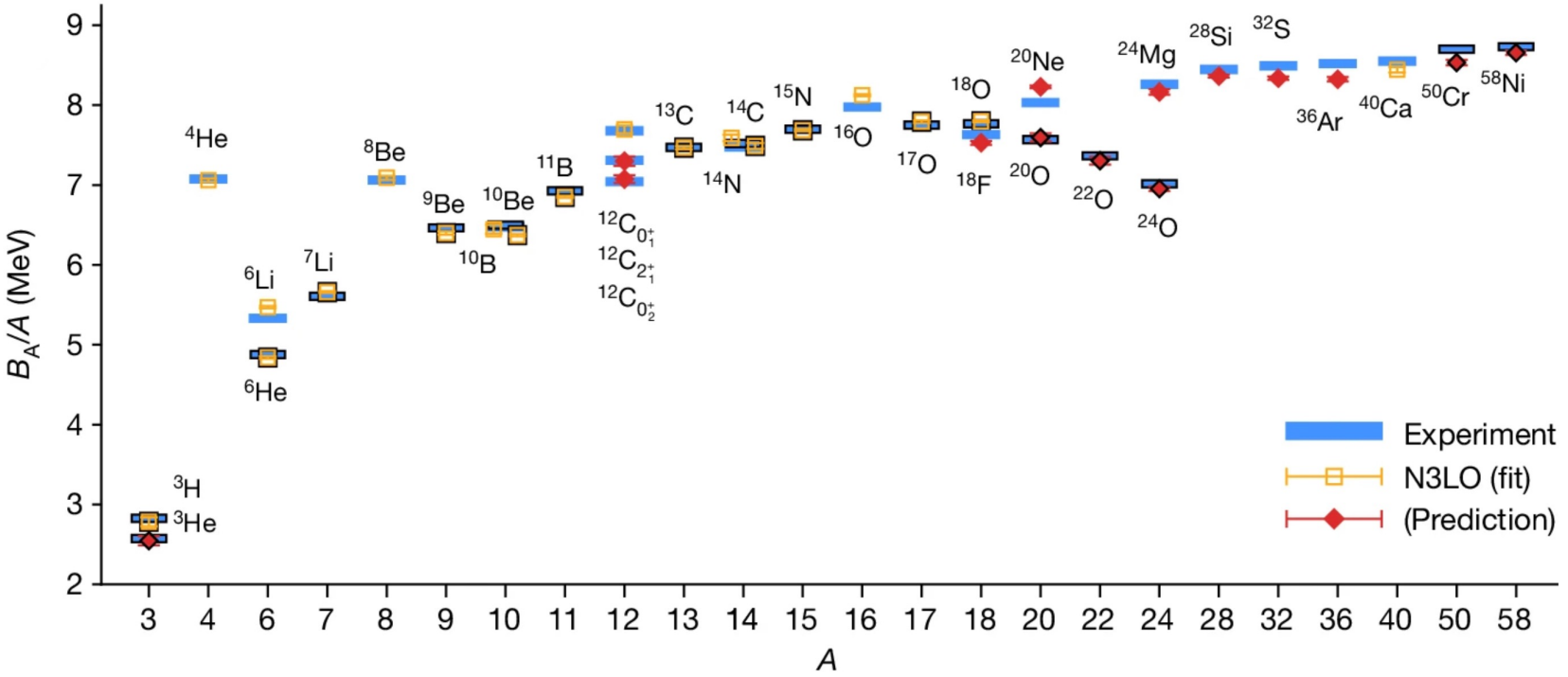

Elhatisari, Bovermann, Ma, Epelbaum, Frame, Hildenbrand, Krebs, Lähde, D.L., Li, Lu, M. Kim, Y. Kim, Meißner, Rupak, Shen, Song, Stellin, Nature 630, 59 (2024)

Charge radii

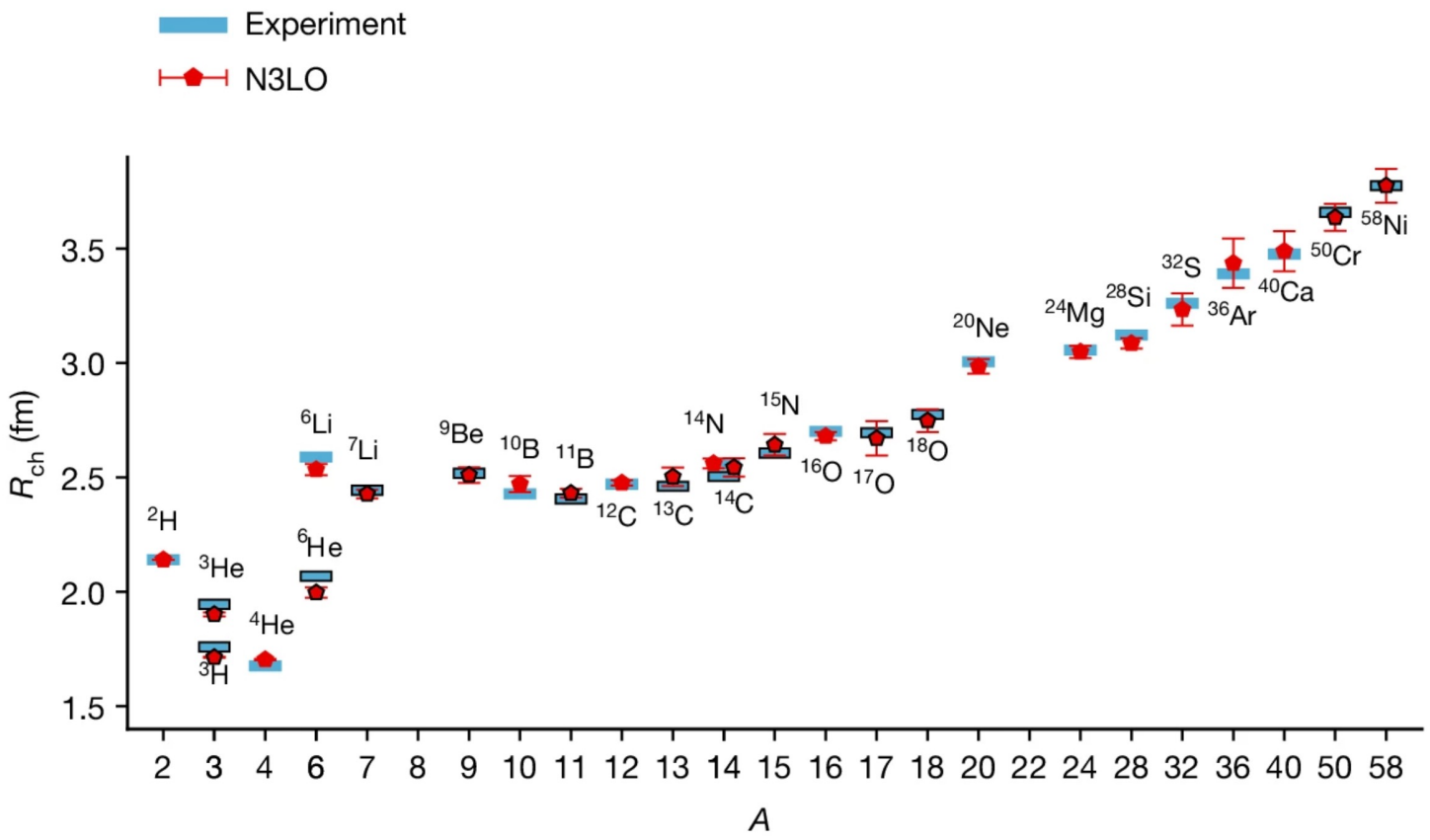

Elhatisari, Bovermann, Ma, Epelbaum, Frame, Hildenbrand, Krebs, Lähde, D.L., Li, Lu, M. Kim, Y. Kim, Meißner, Rupak, Shen, Song, Stellin, Nature 630, 59 (2024)

Charge radii of silicon isotopes

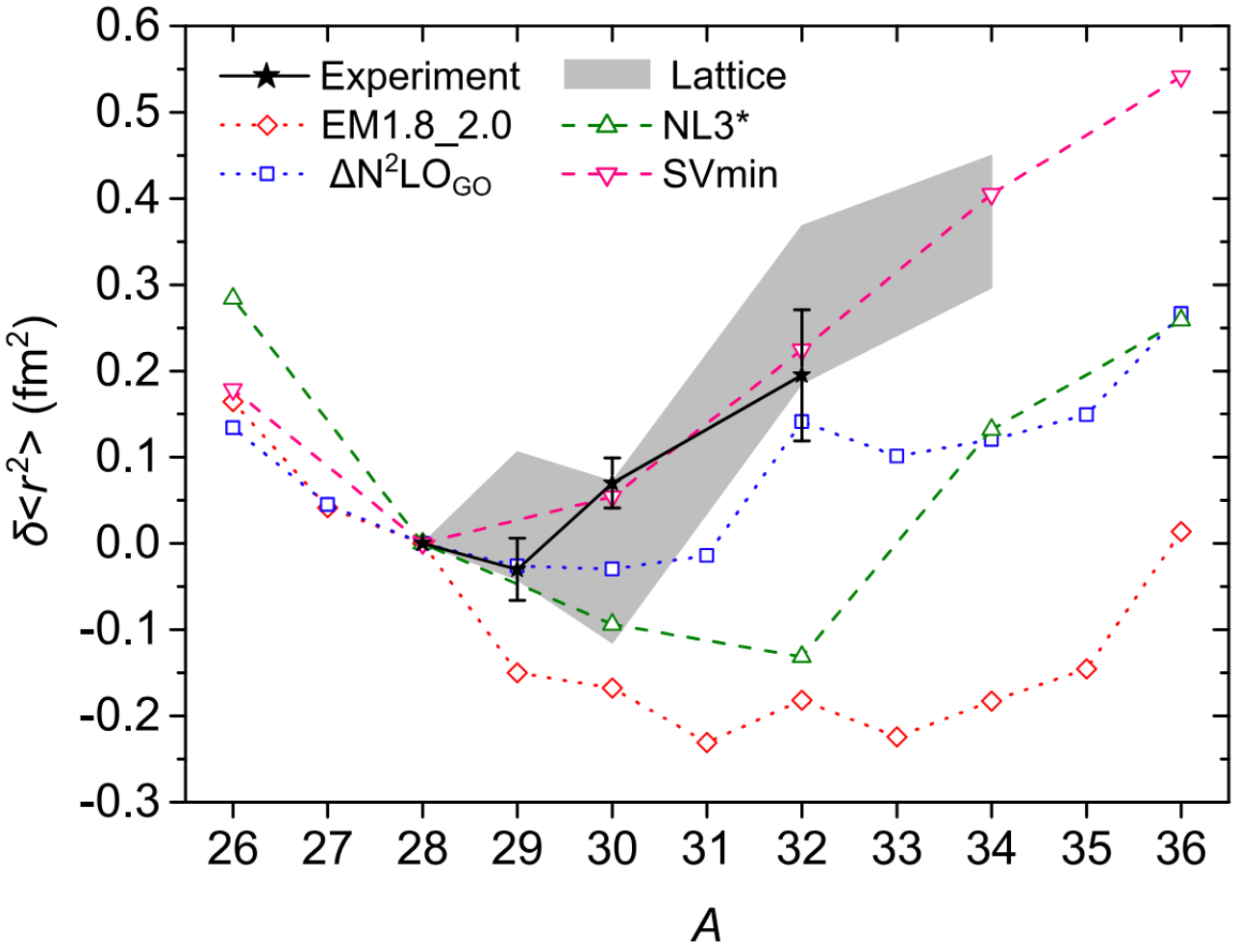

K. König et al., PRL 132, 162502 (2024)

Superfluidity

BEC Theory

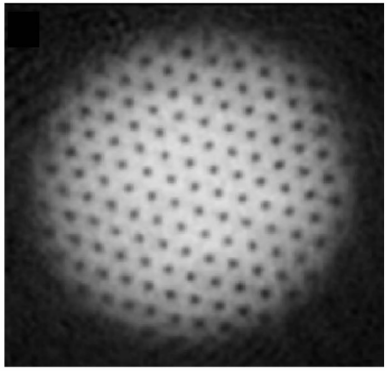

Ketterle, Zwierlein,
Ultracold Fermi Gases (2008)

BCS Theory

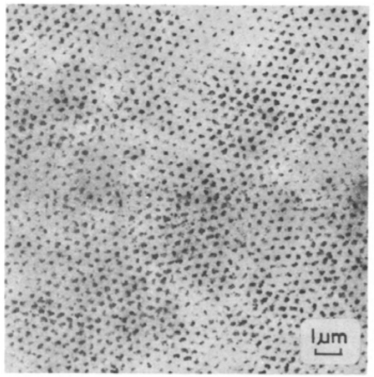

Essmann, Träuble,
Physics Letters A 27, 3 (1968)

Off-diagonal long-range order

Bosonic superfluidity

$$\langle \Psi_0 | a^\dagger(\mathbf{r}) a(\mathbf{0}) | \Psi_0 \rangle$$

Fermionic superfluidity (S-wave)

$$\langle \Psi_0 | a_\downarrow^\dagger(\mathbf{r}) a_\uparrow^\dagger(\mathbf{r}+\Delta\mathbf{r}) a_\uparrow(\Delta\mathbf{r}) a_\downarrow(\mathbf{0}) | \Psi_0 \rangle$$

Fermionic superfluidity (P-wave)

$$\langle \Psi_0 | a_\uparrow^\dagger(\mathbf{r}) a_\uparrow^\dagger(\mathbf{r}+\Delta\mathbf{r}) a_\uparrow(\Delta\mathbf{r}) a_\uparrow(\mathbf{0}) | \Psi_0 \rangle$$

Yang, RMP **34**, 694 (1962)

Multimodal superfluidity

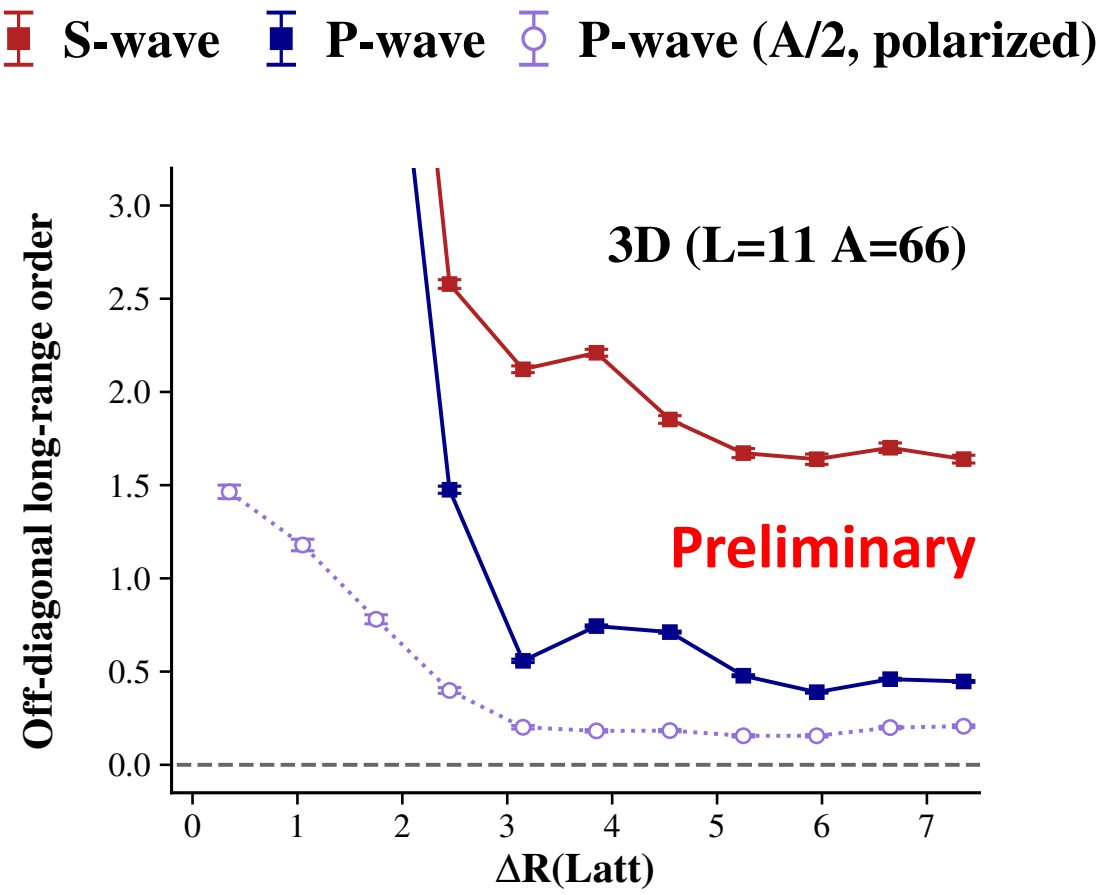

Ma, Palkanoglou, *et al.*, work in progress

Connections to ion collisions at the LHC

Pinhole configurations

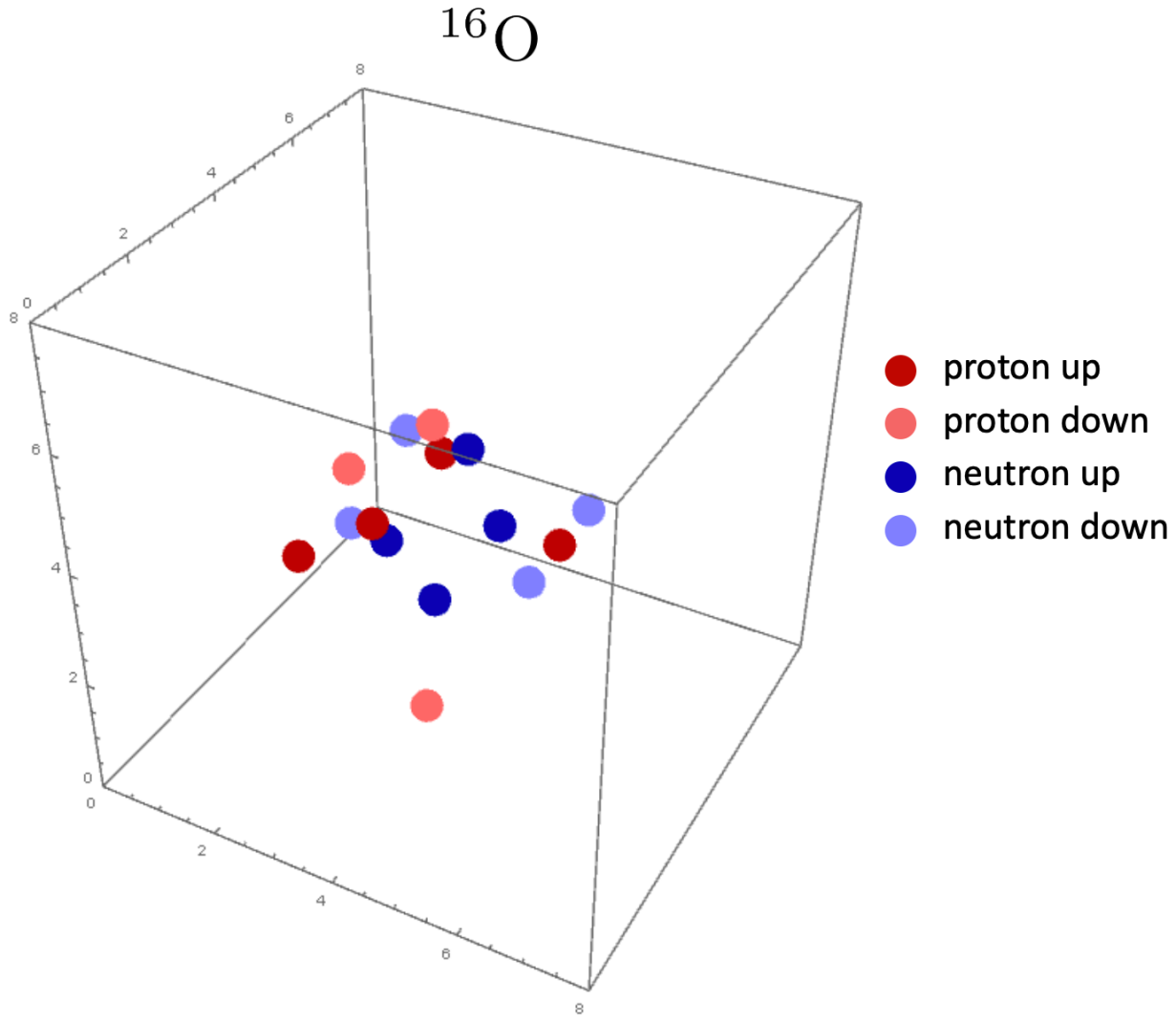

^{16}O

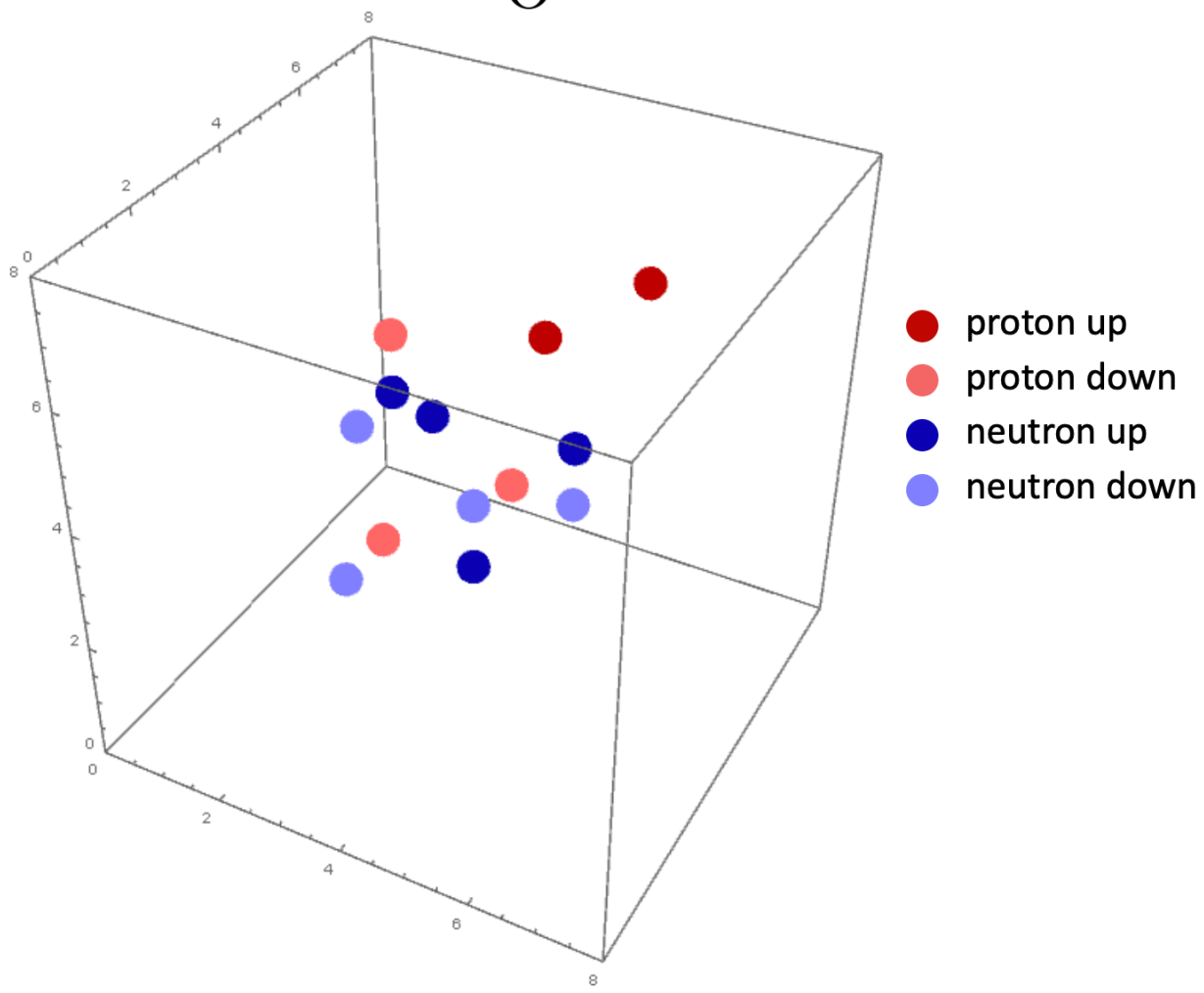

$^{16}O^{16}O$ collisions

$^{16}O^{16}O$ collisions have been performed at RHIC and are planned for LHC Run 3 in June 2025. We used the Trento model to general the initial entropy distribution. The initial entropy distribution is then passed through a free-streaming phase and used to initialize the hydrodynamics evolution. We compute cumulants of the flow harmonics.

$$v_n\{2\} = \left[\left\langle v_n^2 \right\rangle\right]^{\frac{1}{2}}$$
$$v_n\{4\} = \left[2\left\langle v_n^2 \right\rangle^2 - \left\langle v_n^4 \right\rangle\right]^{\frac{1}{4}}$$

We first compute results taking the initial density as a Woods-Saxon potential. We then consider the same Woods-Saxon potential, taking into account the quark substructure of the nucleons. Lastly, we consider using the nucleon distribution from NLEFT calculations.

Summerfield, Lu, Plumberg, D.L., Noronha-Hostler, Timmins PRC 104, L041901 (2021)

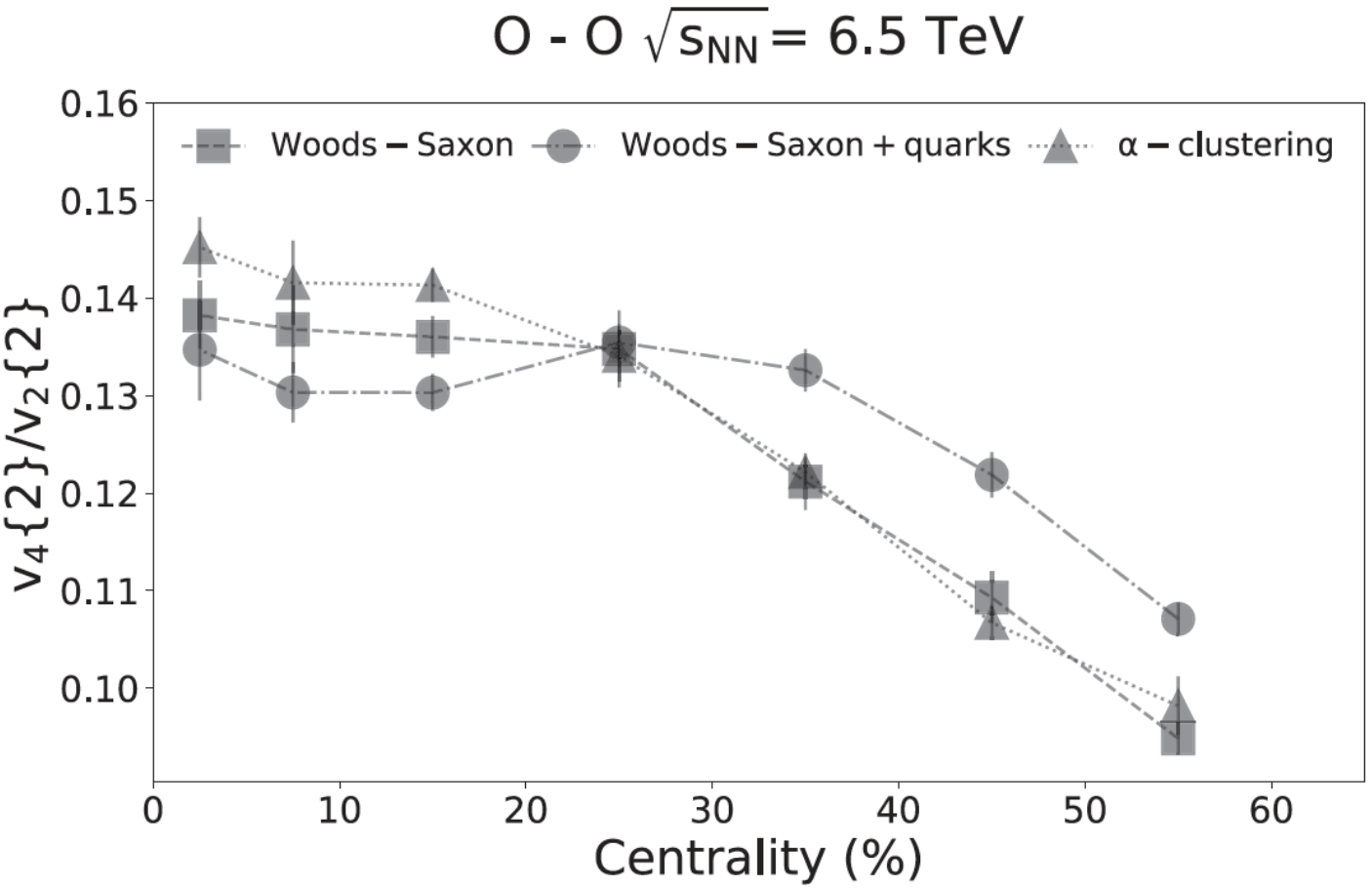

Summerfield, Lu, Plumberg, D.L., Noronha-Hostler, Timmins PRC 104, L041901 (2021)

STAR Collaboration Data for $^{16}O^{16}O$ collisions

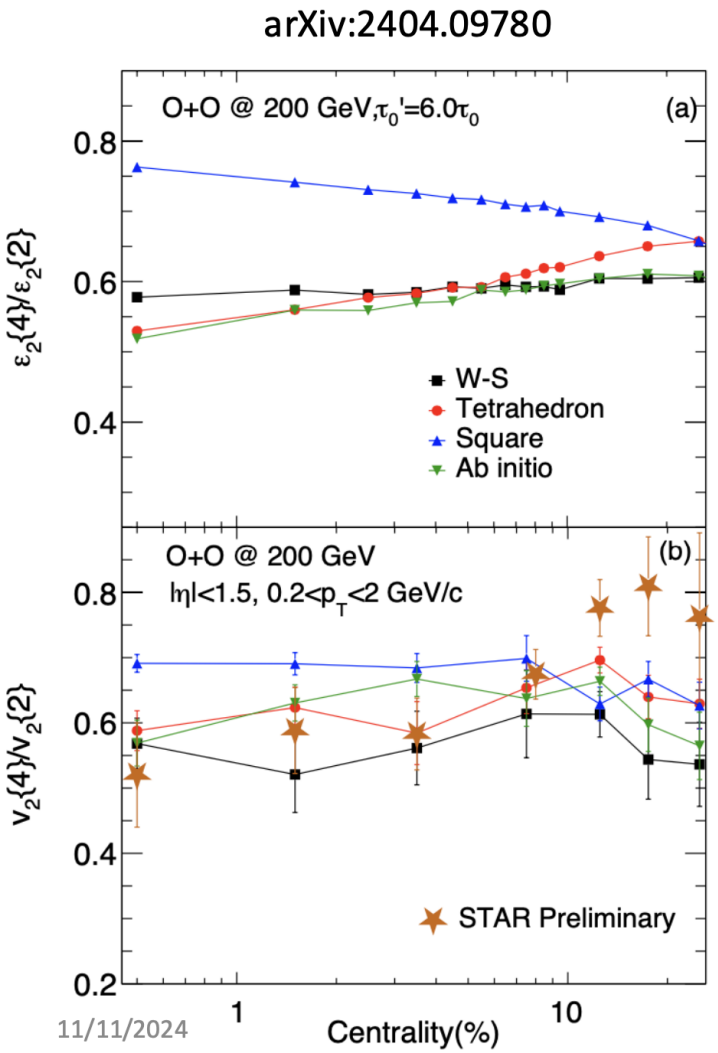

Huang, Monday, Nov. 11

$^{16}O^{16}O$ versus $^{20}Ne^{20}Ne$ collisions

Benjamin Bally

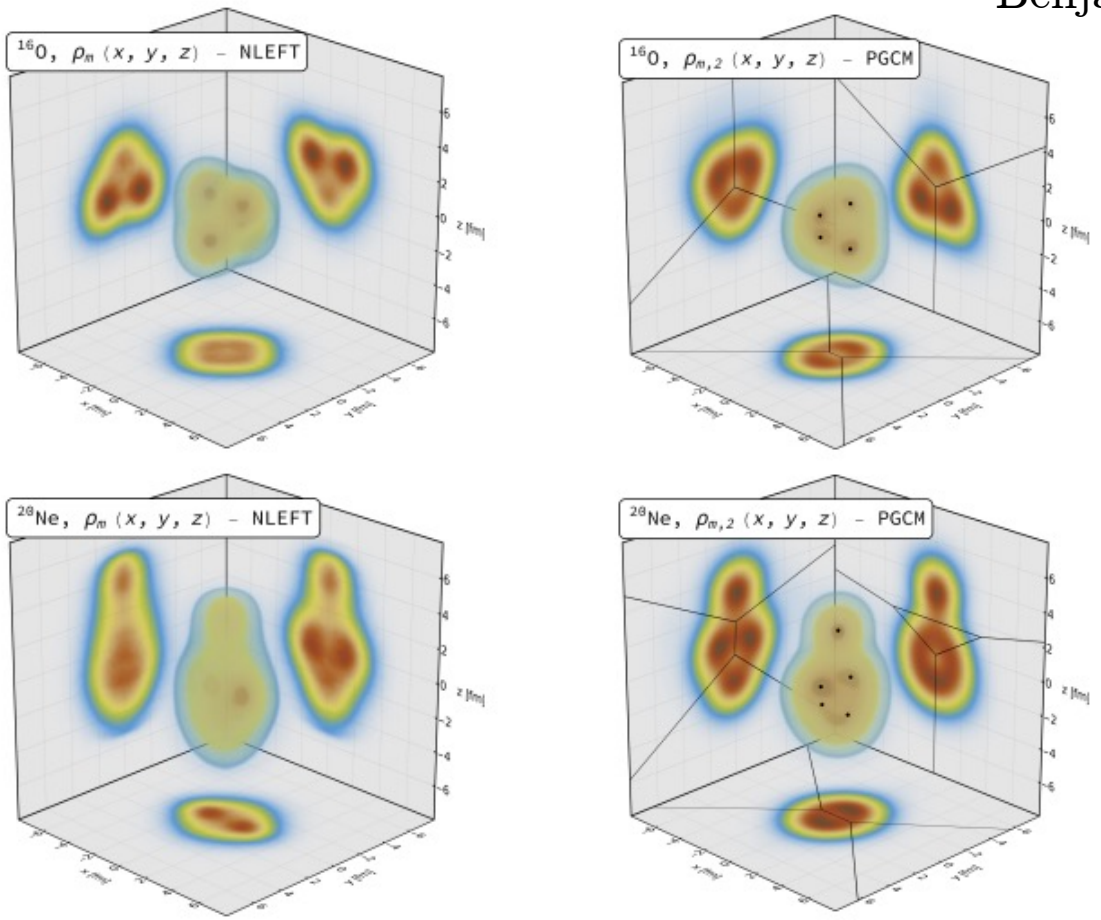

Giacalone, Bally, Nijs, Shen, Duguet, Ebran, Elhatisari, Frosini, Lähde, Lee, Lu, Ma, Meißner, Noronha-Hostler, Plumberg, Rodríguez, Roth, van der Schee, Somà, arXiv:2402.05995

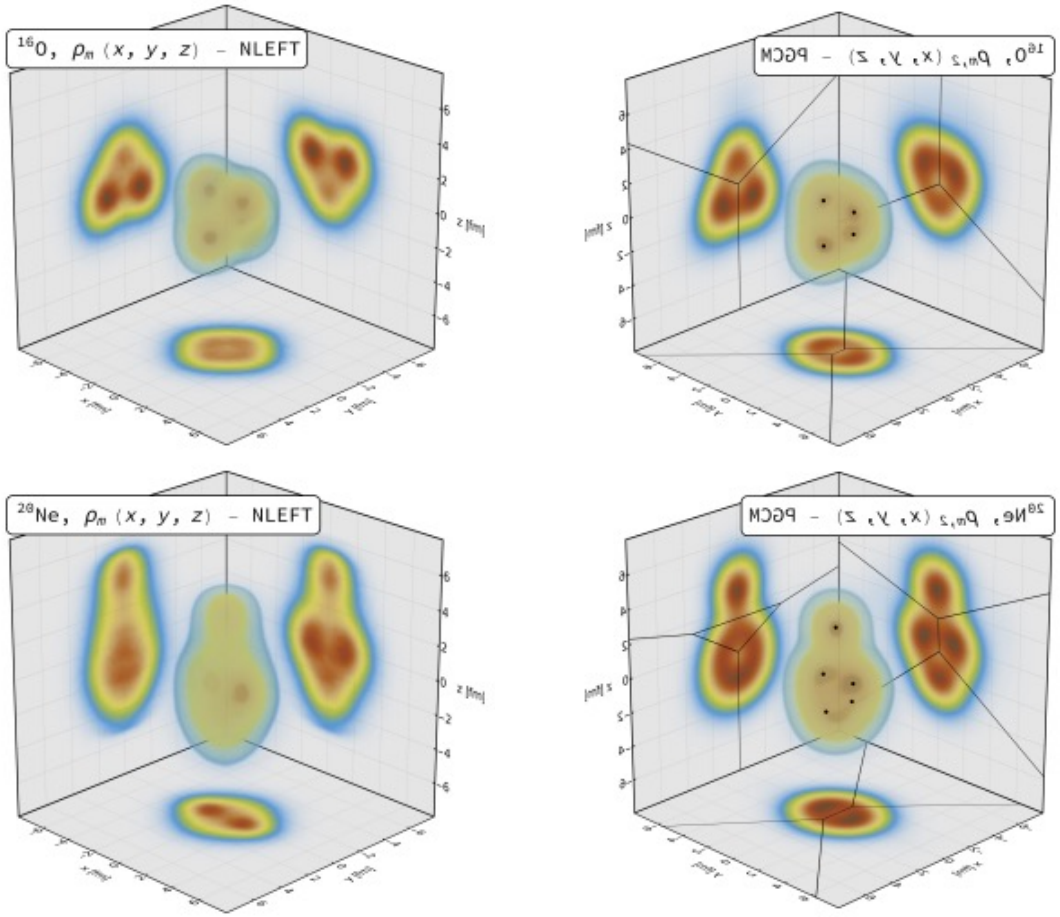
^{16}O, $\rho_m(x, y, z)$ – NLEFT
^{16}O, $\rho_{m,2}(x, y, z)$ – PGCM
^{20}Ne, $\rho_m(x, y, z)$ – NLEFT
^{20}Ne, $\rho_{m,2}(x, y, z)$ – PGCM

We perform event-by-event hydrodynamic simulations of ^{20}Ne^{20}Ne and ^{16}O^{16}O collisions using the Trajectum framework. The calculations start with configurations of nucleons in the colliding nuclei, taken from either the PGCM or the NLEFT results. For the 1% most central events, the elliptic flow of ^{20}Ne^{20}Ne collisions relative to ^{16}O^{16}O collisions is enhanced by as much as

1.170(8)stat.(30)syst. for NLEFT
1.139(6)stat.(39)syst. for PGCM

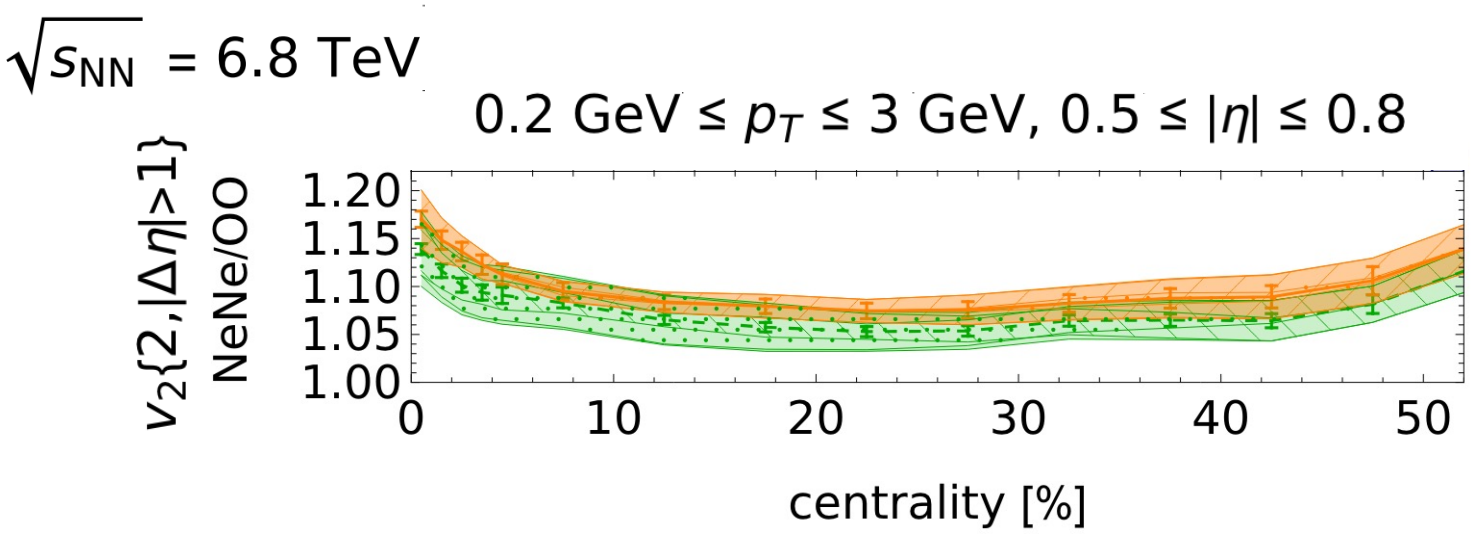

Giacalone, Bally, Nijs, Shen, Duguet, Ebran, Elhatisari, Frosini, Lähde, Lee, Lu, Ma, Meißner, Noronha-Hostler, Plumberg, Rodríguez, Roth, van der Schee, Somà, arXiv:2402.05995

$^{208}Pb^{16}O$ versus $^{208}Pb^{20}Ne$ collisions

Fixed target experiment at LHCb

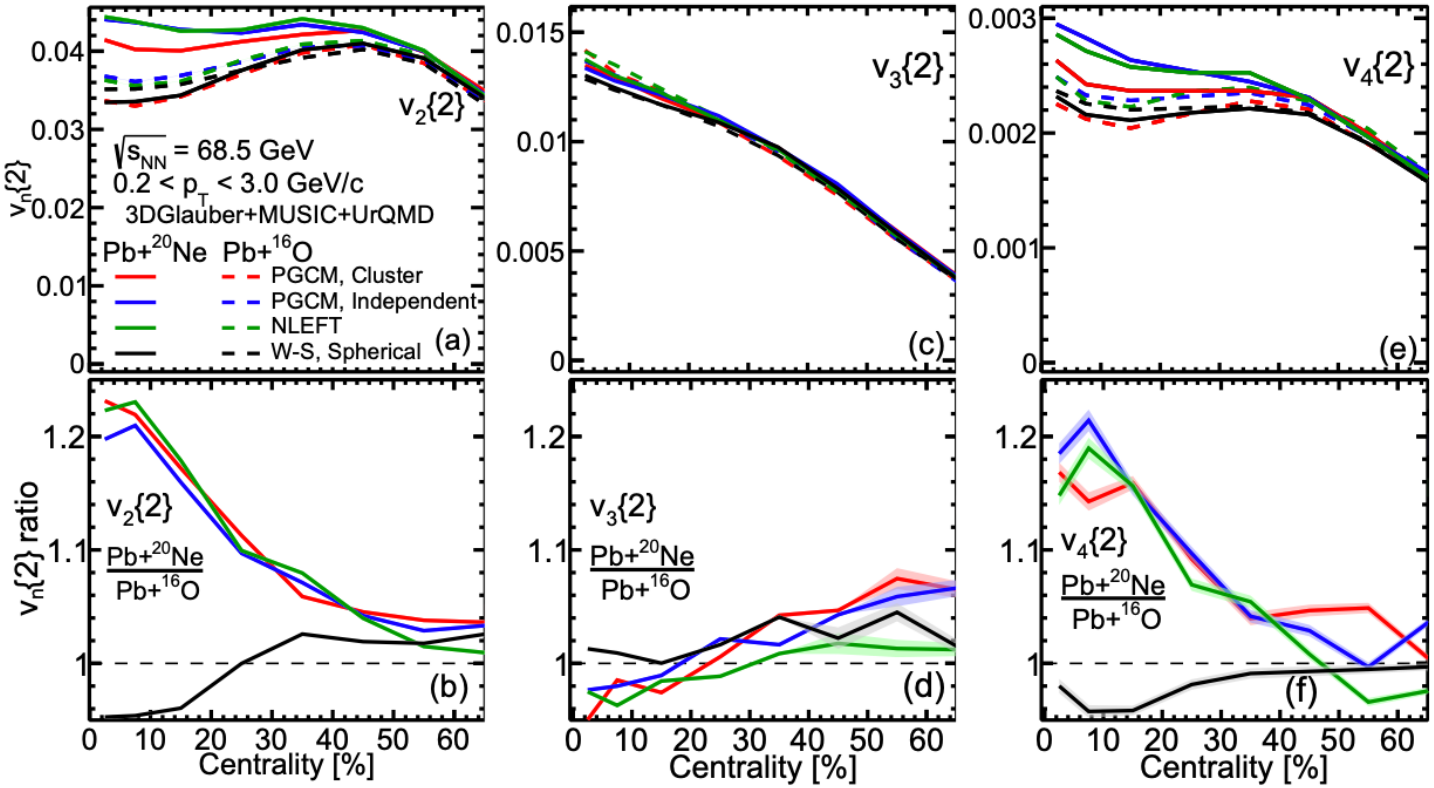

Giacalone, Zhao, Bally, Shen, Duguet, Ebran, Elhatisari, Frosini, Lähde, Lee, Lu, Ma, Meißner, Nijs, Noronha-Hostler, Plumberg, Rodríguez, Roth, van der Schee, Schenke, Shen, Somà, arXiv:2405.20210

Summary and outlook

This talk started with an overview of the *Light ion collisions at the LHC* workshop. It then reviewed several *ab initio* nuclear theory methods, including NLEFT. After this, we discussed recent theoretical developments and described how pinhole configurations provide correlated *ab initio* initial states for relativistic ion collisions.

In several years, it may be possible to do *ab initio* calculations of nuclear states across much of the nuclear chart using NLEFT. We look forward to collaborating with our colleagues working on relativistic ion collisions to explore exciting science while bringing the two nuclear science communities together.